

Variation in Center of Mass Estimates for Extant Sauropsids and its Importance for Reconstructing Inertial Properties of Extinct Archosaurs

VIVIAN ALLEN, HEATHER PAXTON, AND JOHN R. HUTCHINSON*

Department of Veterinary Basic Sciences, Structure and Motion Laboratory,
The Royal Veterinary College, University of London, Hatfield, Hertfordshire, United Kingdom

ABSTRACT

Inertial properties of animal bodies and segments are critical input parameters for biomechanical analysis of standing and moving, and thus are important for paleobiological inquiries into the broader behaviors, ecology and evolution of extinct taxa such as dinosaurs. But how accurately can these be estimated? Computational modeling was used to estimate the inertial properties including mass, density, and center of mass (COM) for extant crocodiles (adult and juvenile *Crocodylus johnstoni*) and birds (*Gallus gallus*; junglefowl and broiler chickens), to identify the chief sources of variation and methodological errors, and their significance. High-resolution computed tomography scans were segmented into 3D objects and imported into inertial property estimation software that allowed for the examination of variable body segment densities (e.g., air spaces such as lungs, and deformable body outlines). Considerable biological variation of inertial properties was found within groups due to ontogenetic changes as well as evolutionary changes between chicken groups. COM positions shift in variable directions during ontogeny in different groups. Our method was repeatable and the resolution was sufficient for accurate estimations of mass and density in particular. However, we also found considerable potential methodological errors for COM related to (1) assumed body segment orientation, (2) what frames of reference are used to normalize COM for size-independent comparisons among animals, and (3) assumptions about tail shape. Methods and assumptions are suggested to minimize these errors in the future and thereby improve estimation of inertial properties for extant and extinct animals. In the best cases, 10%–15% errors in these estimates are unavoidable, but particularly for extinct taxa errors closer to 50% should be expected, and therefore, cautiously investigated. Nonetheless in the best cases these methods allow rigorous estimation of inertial properties. Anat Rec, 292:1442–1461, 2009. © 2009 Wiley-Liss, Inc.

Key words: center of mass; biomechanics; sensitivity analysis; computer modeling; archosaur; dinosaur; bird; locomotion

Grant sponsor: BBSRC; Grant numbers: BB/C516844/1; BB/F01169/1.

*Correspondence to: John R. Hutchinson, Structure and Motion Laboratory, Hatfield, Hertfordshire AL9 7TA, United Kingdom. Fax: 44-1707-666-371. E-mail: jrhutch@rvc.ac.uk

Received 9 June 2009; Accepted 9 June 2009

DOI 10.1002/ar.20973

Published online in Wiley InterScience (www.interscience.wiley.com).

An animal's body mass, or the mass of any of its component segments, can be abstracted as having a center of mass (COM) located at some point within or near it. The COM along with mass and inertial tensor values are typically grouped as "inertial (or mass) properties," (used here) "inertial parameters," "body segment parameters," or "mass sets." Like all inertial properties, accurate knowledge of animal COM is critical for the analysis of posture, gait, energetics, and other biological phenomena (e.g., Cavagna et al., 1977; Fedak et al., 1982).

COM positions alone are valuable for predicting locomotor/dynamic performance variables (e.g., turning or running speed) and other ecologically-relevant factors (Srygley and Dudley, 1993). An excellent example is the study by Clemente et al. (2008), which showed how COM proximity to the hips in extant lizards is strongly correlated with bipedal running ability. This value extends into paleobiological questions, such as the role of segment inertia in feeding (Snively and Russell, 2007) and turning (Carrier et al., 2001; Henderson and Snively, 2004; Hutchinson et al., 2007) behaviors of large tyrannosaurs, or ontogenetic changes in posture in smaller dinosaurs (Heinrich et al., 1993; Reisz et al., 2005).

Yet relative to other inertial properties, the accuracy of COM estimation has often been neglected, especially with reference to studies of extinct taxa. Here, we analyze natural and methodological (i.e., error) variation in COM estimates for extant archosaurs (crocodilians and birds). We aim to phylogenetically bracket (loosely applied) how much variation of COM values might be expected for extinct archosaurs, especially non-avian dinosaurs.

By far the most effort in measuring or estimating COM values has been invested in human-based biomechanical or ergonomic studies, using mechanical balancing, cadaver-based regressions, photogrammetry, or geometrical modeling (Dempster and Gaughran, 1967; Jensen, 1978; Hatze, 1980; Lephart, 1984; Yeadon, 1990; Sarfaty and Ladin, 1993; Baca, 1996; de Leva, 1996; Challis, 1999; Dumas et al., 2007). Scanning techniques are also widely used, including gamma scanning (Zatsiorsky and Seluyanov, 1983), dual X-ray absorptiometry (Wicke et al., 2008), laser surface scanning (Norton et al., 2002), magnetic resonance imaging (Mungiole and Martin, 1990), and computed tomography [(CT); Huang and Suarez, 1983; Wei and Jensen, 1995].

Studies of inertial properties, such those that include COM measurements, have incomplete coverage for non-human species. Manion (1984) estimated COMs for chickens across their ontogeny by suspending them from three different points and overlaying photographs to find COM coordinates relative to landmarks. He found that COMs shifted cranioventrally from 5 to 19 days of age. During this time, the pectoral limbs grew and limb orientation became more flexed during standing, but more extended during walking. Similar kinds of suspension/pendulum-based techniques, occasionally combined with geometric modeling or regression equations, are by far the most common methods used for other species (e.g., in Fedak et al., 1982; Walter and Carrier, 2002), especially primates (Crompton et al., 1996; Isler et al., 2006), horses (van den Bogert et al., 1989; Buchner et al., 1997), elephants (Ren and Hutchinson, 2008), and birds (Hutchinson, 2004; Goetz et al., 2008).

Recently, dinosaur researchers have estimated dinosaur COMs to reconstruct their locomotor biomechanics. Alexander (1985) used physical models to show that dinosaur COMs were positioned cranioventral to the hips, which enabled the estimation of fore and hind limb bone loadings. Henderson (1999) provided a major improvement by implementing 3D body reconstructions in computer models to estimate COMs for large dinosaurs and also, for validation of the technique, extant large mammals. He subsequently conducted similar analyses for various sauropods (Henderson, 2004, 2006) as well as theropods and other bipedal archosaurs (Henderson and Snively, 2004), which included brief sensitivity analyses of unknowns such as mediolateral body dimensions. Heinrich et al. (1993), Jones et al. (2000), and Christiansen and Bonde (2002) reconstructed COMs for a small group of dinosaurs using simple models, but like many previous studies, did not present quantitative data. Like Gunga et al. (2007), Bates et al. (2009) used laser-scanning of whole dinosaur skeletons to build whole-body models, and (unlike Gunga et al., 2007) estimate inertial properties.

Hutchinson et al. (2007) built deformable B-spline solid computer models of an ostrich carcass, for procedural validation, and an adult *Tyrannosaurus rex*, for sensitivity analysis of COM and other parameters to estimate turning and running biomechanics (this included 30 different models of *T. rex* anatomy). The latter study quantified errors/variation in COM values, finding that the total body COM for a representative adult *T. rex* was 0.45–0.74 m cranial and 0.229–0.335 m ventral to the hips (~0.5 and ~0.25 femur segment lengths cranioventral). Air sac dimensions had small effects on COM, whereas tail (and pelvic limb) dimensions had proportionately large effects. Bates et al. (2009) also performed a very similar sensitivity analysis, with similar results.

Motani (2001) noted that the assumptions of an elliptical body cross section by Henderson (1999 and later) and other studies could not only introduce inaccuracies in estimating mass but also COM, perhaps causing a caudad directional bias of COM position due to underestimation of body mass in the cranial half of the body. Also, he observed that cross-sectional profiles of animal body segments diverge significantly in size and shape from their underlying skeletal scaffold. Especially in taxa with long tails, this has the potential to be an important source of uncertainty for COM position estimates.

Yet to date there has been little study of the accuracy of quantifying COM and other inertial properties for extant taxa (except for humans and a few other species) from the underlying anatomy alone (refer Hutchinson et al., 2007 and Bates et al., 2009 for simple examples with ostriches), or the individual variation amongst the same age cohort or across ontogeny. As COM has critical importance for behaviors of broad paleobiological interest, such as bipedalism/rearing, gait mechanics, ontogenetic shifts, and flight, there are unresolved concerns about the expected variability and accuracy of inertial property estimates for extinct taxa.

Here, for extant archosaurs, we characterize the degree of COM variation (1) among conspecific individuals of the same size, (2) during growth (using ontogenetic sequences) and evolution (using related breeds), (3) due to errors in estimating COM values (e.g., resolution

of imaging technologies, human measurement error, frames of reference for reporting COM values, and limb/body segment orientations), and (4) with estimates in a best case scenario for extant taxa [e.g., effects of assumptions ca. body outlines beyond skeletal indicators (especially in the tail; Motani, 2001), and air spaces within the body that alter regional densities]. This has direct implications for COM estimates in extinct taxa, particularly those with long tails such as archosaurs, for which COM values will forever be unknown parameters. As mass and density are related to COM and are calculated in its estimation, we additionally compare the accuracies of estimating mass and density versus calculating them using computational methods. By quantifying the amount of natural variation versus “methodological variation” of inertial properties for extant taxa, we will better appreciate how closely we can estimate these values for extinct taxa and thereby inform future biomechanical and evolutionary analyses.

MATERIALS AND METHODS

To acquire 3D geometry of animal bodies necessary for COM estimation, we used CT scanning of cadaveric specimens. All scans took place at The Royal Veterinary College’s Hawkshead campus, using a Picker PQ5000 CT scanner. We focused on crocodylians and birds (extant Archosauria). For crocodylians, we CT scanned one juvenile (body mass 1.54 kg) and one adult (body mass 20.19 kg) Australian freshwater crocodile (*Crocodylus johnstoni*), ages unknown. Specimens had died naturally in captivity and were free from pathologies that would influence our results. We obtained the adult crocodile in three sections (head, torso/limbs, and tail) that were scanned separately and digitally reconnected in MIMICS 11.0 imaging software (Materialise; Leuven, Belgium).

For birds, we CT scanned 15 domestic chickens (*Gallus gallus*): ten 4-week old (body mass 1.99 ± 0.16 kg) and five “mature” (morphologically subadult, but at slaughter age) 6-week old specimens of Cobb 500 broilers (body mass 2.79 ± 0.22 kg). Broilers are bred for extreme anatomy related to large pectoral muscle mass, and in terms of unusual body shape thus are a “worst case” example for estimating inertial properties. In addition, to represent the more natural ancestral morphotype from which broiler chickens evolved (Fumihito et al., 1994; Liu et al., 2006), we CT scanned five (6-week old; body mass 0.60 ± 0.074 kg) juvenile and five adult (15-week old; body mass 1.94 ± 0.15 kg) giant junglefowl. Junglefowl and broiler chickens here are discussed together as “chickens.” Chickens were obtained as byproducts of normal culling and did not have pathologies that would influence our main results here.

Animals were placed with their ventral surface resting on a radiolucent cushion. Limbs were posed as similarly as possible for each species (Figs. 1 and 2), to minimize postural effects on COM estimates. However, in all cases due to scanner constraints and the imprecision of posing limbs manually, precise positioning of the limbs and body was not possible among specimens—we return to this critical point in the Results and Discussion. The specimens were then scanned with axial 512×512 pixel CT slices at 100 mA and 120 kVp X-ray beam inten-

sities. Details on CT scan slice thicknesses and resolutions are presented in Table 1.

CT scans were converted to DICOM images and imported into MIMICS 11.0 imaging software (Materialise; Leuven, Belgium) for segmentation and 3D reconstruction. Images were semiautomatically thresholded into 3D volumes using grayscale values (involving some manual adjustment from baseline values) and exported as DXF, OBJ, STL, or ASC format 3D computer graphics images. These then were imported into custom inertial property measurement software (Hutchinson et al., 2007). In the latter software we either used the raw segmented geometry (original models) with homogeneous density (as below) or constructed a simplified framework of deformable b-spline solids (as in Hutchinson et al., 2007), one per body segment. These b-spline solids allowed for deformation of the body surface (e.g., to simulate the reconstruction of body outlines from skeletal landmarks alone) and embedding of zero-density objects (e.g., lungs and other air spaces). To examine the accuracy of this procedure, we modeled the same individual (an adult junglefowl, discussed further below for a sensitivity analysis of air space dimensions) using both the detailed original segmentation (which did not allow embedded air spaces or easy deformation of tissues) and the simplified b-spline solid geometry (which did allow such modifications).

The 3D geometric objects representing flesh were given densities equivalent to water (1000 kg m^{-3}), whereas those representing air spaces were given zero density (a reasonable approximation for the empty cavities; Hutchinson et al., 2007). In our original models of crocodiles and chickens (Tables 1–3), we excluded the air spaces entirely, but we compared actual body masses with estimated masses to determine the effects of this assumption. In later, detailed models (Tables 4 and 5), we included air spaces directly segmented from the cavities evident in CT scans.

COM positions along the x (craniocaudal; positive = cranial), y (dorsoventral; positive = dorsal), and z axes (mediolateral; positive = right lateral) were calculated by the inertial properties software for the input geometry and densities, and expressed relative to the location of the right hip joint (following Hutchinson et al., 2007; Figs. 1 and 2). Note that the z-coordinate value is the distance from the body midline and thus is about half of the distance between the right and left hip joint centers. Values were then expressed with four different frames of reference to normalize them for cross-taxa comparisons, therefore removing size effects: (1) body mass^{0.33} (perhaps an ideal method to non-dimensionalize COM values as it is more independent of individual body dimensions that might themselves vary separately from COM variation); (2) femur length (following Hutchinson et al., 2007 and related studies); (3) body length (snout to tail tip with body straightened); and (4) limb length (center of femoral head to middle of third metatarsophalangeal joint; sum of all bone lengths if limb were extended vertically).

Different normalizing factors had distinct advantages and demerits. Body mass^{0.33} seems an ideal parameter for normalizing COM (as it by definition scales isometrically with size), but it is less well-constrained for extinct taxa than femur length or limb or body length. Body length is a simple metric to apply. Alternatively, femur

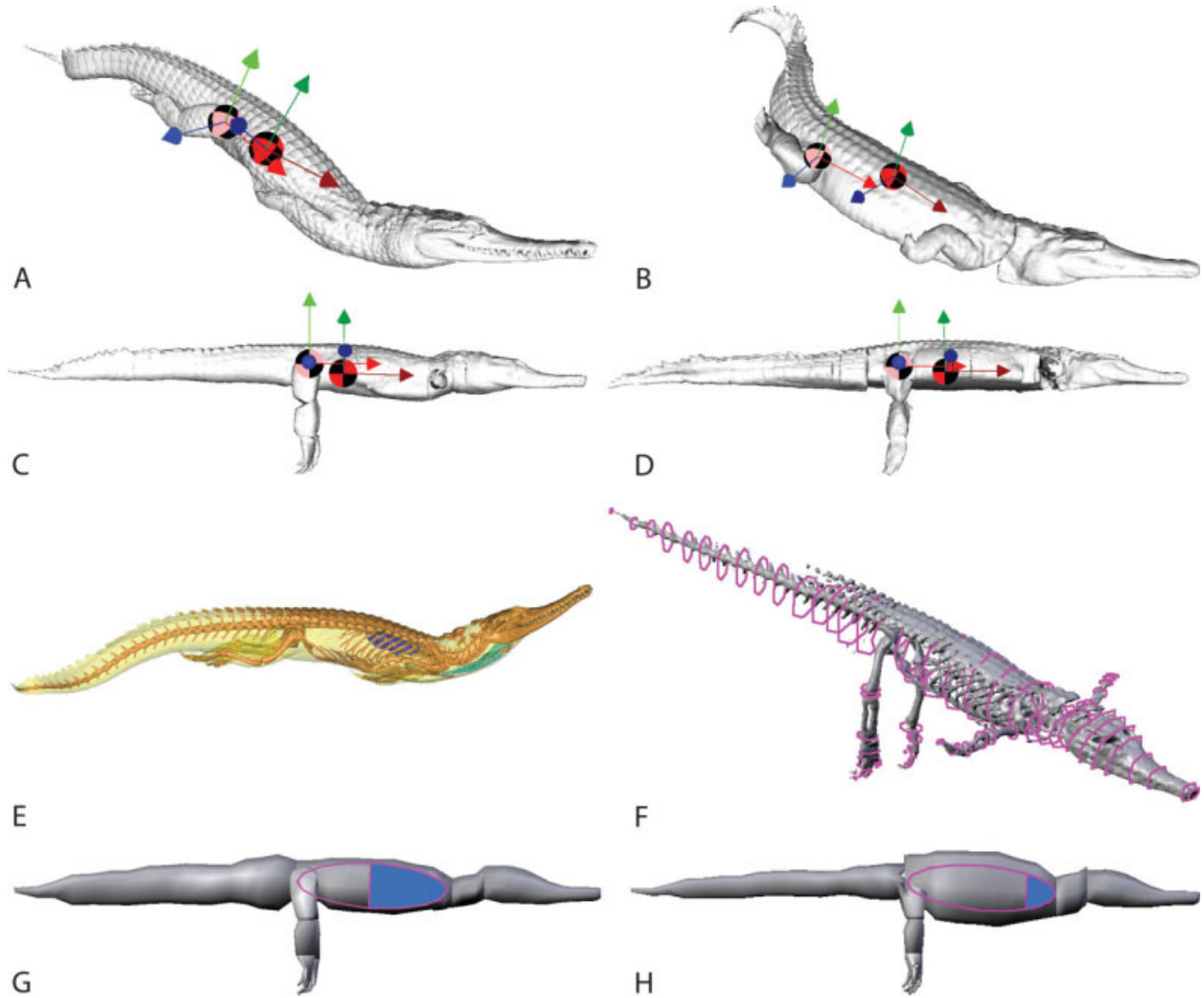


Fig. 1. Australian freshwater crocodile (*Crocodylus johnstoni*) models used for inertial properties calculations, in right lateral view (corresponding to data in Tables 1, 2, and 5). Not to scale; scaled to same total length where relevant—refer Table 1 for measurements. Pink disc represents right hip’s reference point; red disc shows center of mass. Axes shown are x (cranial; red), y (dorsal; green), and z (lateral; blue). Original, unstraightened models from original scan positions: **A**, juvenile; **B**, adult. “Straightened, detailed” models in reference pose (trunk only COMs in Table 2 corresponds to these models with limbs omitted): **C**, juvenile; **D**, adult. **E**, Original scan of juvenile crocodile in right

lateral view, showing air cavities (dark blue = lung; light blue = pharyngeal/cranial cavities) used in “realistic” models (Table 5). **F**, “Simplified” modeling procedure using skeletal dimensions alone to estimate inertial properties; juvenile crocodile shown in right oblique view. The purple hoops correspond to anatomical landmarks and were deformed by set amounts to extend the flesh beyond the skeleton. Simplified models of juvenile crocodile to illustrate the COM estimates in Table 5: **G**, “Max caudal” model; **H**, “Max cranial” model (refer Methods). Purple ellipse represents thoracic cavity boundaries; blue filled section represents thoracic cavity (zero density) area in each model.

or limb length can have greater functional relevance. For example, the femur must be sufficiently long to position the knee cranially to the COM to allow for bipedal stability, and limb length must be adequate to permit placement of the foot under the COM (e.g., Hutchinson, 2004; Hutchinson et al., 2007). Certainly for extinct taxa, body length or especially femur and limb length are more directly measurable than body mass.

In addition, the craniocaudal position of the right hip joint as a fraction of body length was examined for comparison to these factors, to provide a more complete picture of how different ways of reporting COM positions might influence broader conclusions, and to assess the

reliability of using the right hip as a reference point. COM estimates were expressed for the whole body (including limbs) and trunk only (pelvic limbs removed at their proximal joints in MIMICS software; Fig. 3). This COM estimation avoided the problems inherent in the variable pelvic limb poses. It was also conducted for the crocodile models.

For investigation of potential errors in COM position estimates, we CT scanned one adult broiler chicken and one junglefowl at lower (3.0 mm slice thickness) and higher (1.5 mm slice thickness) longitudinal resolution. Between scans, the broiler chicken specimen was removed, so its pose was only roughly consistent among

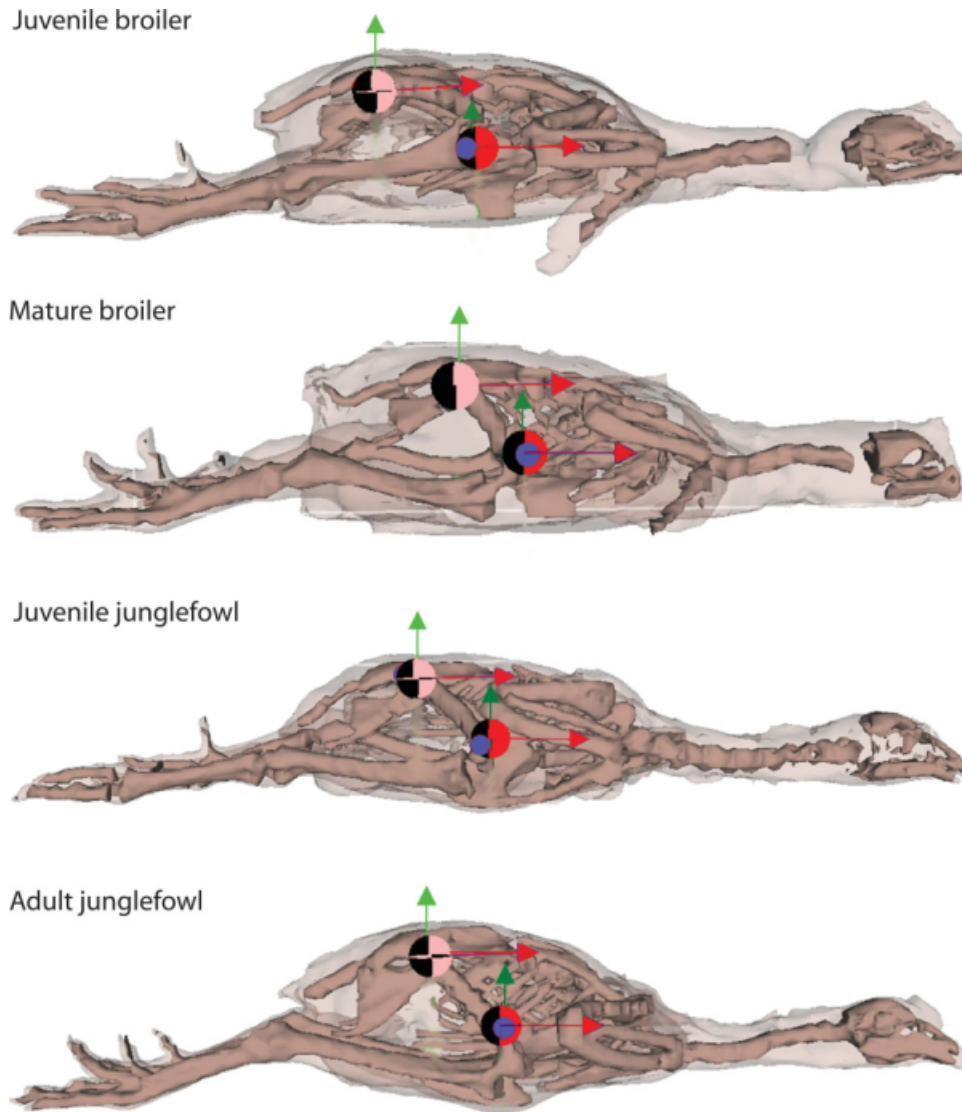


Fig. 2. Chicken (*Gallus gallus*) models, in right lateral view, corresponding to cohorts in Table 1. Not to scale; scaled to same total length. Labels as in Fig. 1. The skeletons are shown for reference and were not part of inertial properties calculations; the translucent outline represents the “virtual flesh” of the models.

scans. The junglefowl was not disturbed between scans. This again allowed us to check the effects of the limb and head/neck poses used in scanning.

In addition, for one 6-week old broiler chicken we repeated the MIMICS segmentation and COM modeling procedure (above) 5 times to check the effects of this critical step on our COM estimates.

To assess the effects of differing poses on chicken and crocodile inertial properties, we compared results based on the raw scans of specimens in their original poses to those based on specimens which had been re-posed into a straightened “reference pose” by deforming the original scan in Blender 2.47 open source 3D graphics software (www.blender.org). Briefly, the individual vertices that define the 3D geometry of the body were selected in groups representing body segments, and these were rotated into the reference poses displayed in Fig.

1C,D,F–H—forelimbs fully abducted and extended (i.e., oriented along the z-axis), hindlimbs extended fully ventrally, glenoid and acetabulum horizontal, tail fully extended caudally (similar to Hutchinson et al., 2007), and other vertebrae posed in the neutral position suggested by their articular surfaces. As a convention, here, we refer to the initial scanned poses as the “original” models, and inertial properties estimates for reference-poses as the “straightened” models.

To evaluate typical methodology used to estimate inertial properties for extinct taxa (e.g., Henderson, 1999; Hutchinson et al., 2007) we created simplified models in Blender based solely on skeletal landmarks from an adult junglefowl and the juvenile and adult *C. johnstoni*, and then compared estimates of inertial properties based on these simple models to those based on the original scans. The simple models were created in Blender by

TABLE 1. Main archosaurian study specimens—basic information

Parameter	Juvenile broiler	Mature broiler	Juvenile junglefowl	Adult junglefowl	Juvenile crocodile	Adult crocodile
Age (wk)	4	6	6	15	n/a	n/a
N (cadavers)	10	5	5	5	1	1
Actual mean mass ^a	1.99	2.79	0.60	1.94	1.54	20.19
SD	0.16	0.22	0.07	0.15	n/a	n/a
Estimated mass ^b	2.06	2.92	0.66	2.17	1.79	21.3
SD	0.16	0.30	0.09	0.27	n/a	n/a
Estimated/actual mass (%) ^c	103	105	110	112	116	105
Estimated density (kg m ⁻³) ^d	968	953	909	894	860	948
CT slice thickness (mm)	3.0	3.0	1.5	3.0	1.3	2.5
CT resolution (pixels mm ⁻¹)	2.133	1.707	2.560	1.707	2.048	1.024

^aMass from electronic balance (± 0.001 kg).

^bMass from inertial properties estimation software.

^cError = 100*(Estimated mass/Actual mass).

^dModel density of 1,000 kg m⁻³ divided by (estimated/actual mass) from above to estimate actual density of cadaver.

TABLE 2. Center of mass (COM) position normalized by femur length for *Crocodylus* cadavers

Pose	COM position	Juvenile crocodile	Diff. (%)	Adult crocodile	Diff. (%)	Ratio
Original	Cranial x (/femur length)	0.55	0	1.6	0	2.8
Original	Ventral y (/femur length)	-0.24	0	-0.10	0	0.42
Original	Medial z (/femur length)	-0.33	0	-0.96	0	2.9
Straightened	Cranial x (/femur length)	0.92	167	1.2	79	1.3
Straightened	Ventral y (/femur length)	-0.24	100	-0.10	110	0.42
Straightened	Medial z (/femur length)	-0.41	122	-0.51	52	1.2
Trunk only	Cranial x (/femur length)	1.6	297	1.94	124	1.2
Trunk only	Ventral y (/femur length)	-0.22	92	0.010	-10	-0.043
Trunk only	Medial z (/femur length)	-0.41	169	-0.51	52	1.2

“Original” pose is the cadaver scanned in its unstraightened configuration (Fig. 1A,B). “Straightened” pose corresponds to a modified model in the reference posture, with limbs vertically straightened and trunk aligned with the craniocaudal (x) axis (Fig. 1C,D). “Trunk only” corresponds to the straightened model with the limbs removed. Air cavities were still absent in all of these models. The “diff” column is the % difference from the original pose model. The “ratio” column is the ontogenetic ratio of COM position in the adult relative to the juvenile crocodile. Note that this ratio is negative for the “trunk only” model’s ventral COM position because the adult’s COM is 0.010 femur length dorsal to the right hip joint. Juvenile and adult femur lengths were 0.054 m and 0.105 m, respectively. x, cranial; y, ventral; z, medial relative to right hip.

fitting octagonal “hoops” tightly onto the skeleton (Fig. 1F), and lofting (polygon skinning) them to create a “watertight” (i.e., gapless) polygon mesh. The whole-body mesh was divided into eight segments: cranial, cervical (vertebral series from atlas to first dorsal/pectoral vertebra), thoracic/abdominal/pelvic (body from pectoral girdle to pelvic girdle), caudal, two forelimbs, and two hindlimbs.

In these simple models, the lungs were recreated as segments of an ellipsoid fitted closely to the inside of the ribcage (Fig. 1G,H), representing set fractions of the thoracic cavity volume (bounded by ranges observed in extant archosaurs). Smaller airspaces were simply fitted to appropriate skeletal landmarks—the inside of the nasal sinuses for the nasal cavity, the interior margins of the mandible and bony palate for the buccal cavity.

To account for unknowns regarding the true body dimensions of extinct animals, it is now standard to apply a sensitivity analysis to paleontological reconstructions of inertial properties, in which body segment parameters are systematically altered, and the potential range of estimations for inertial properties noted. We

applied a similar sensitivity analysis to our simple models. The radial dimensions of the simple hoops that defined each body segment’s shape were scaled between their initial skeleton-hugging values and +20% to simulate a “minimal” and “maximal” body outline (after Hutchinson et al., 2007). These were then combined to represent the maximum plausible variability in total mass estimates and the most dorsal, ventral, cranial, and caudal positions of the centre of mass—thus bounding the possible range of inertial properties estimates possible. As an example, the “maximal caudal” model simply consists of the largest tail and hindlimbs combined with the smallest chest, neck, and forelimbs and the largest air spaces; the “maximal cranial” model was the opposite (Fig. 1G,H).

We also CT-scanned three lizard cadavers to model the relationship between tail shape and skeletal dimensions, for comparison with archosaurs. These lizard specimens were included because of their more basal phylogenetic position outside Archosauria (Gauthier et al., 1988), polarizing the evolution of tail shape, but were excluded for body COM calculations due to the eviscerated/

TABLE 3. Center of mass (COM) for chicken body and trunk, with normalization methods

COM parameter	Juvenile broiler	Mature broiler	Juvenile junglefowl	Adult junglefowl
COM x (/body mass ^{0.33})	0.035	0.028	0.028	0.039
±SD	0.0027	0.0043	0.0086	0.0048
COM x (/femur length)	0.611	0.502	0.375	0.533
±SD	0.042	0.086	0.11	0.063
COM x (/limb length)	0.177	0.148	0.111	0.150
±SD	0.012	0.027	0.033	0.015
COM x (/body length)	0.121	0.099	0.083	0.113
±SD	0.0086	0.012	0.025	0.012
Trunk COM x (/femur length)	0.927	0.826	0.710	0.787
±SD	0.066	0.11	0.082	0.068
COM y (/body mass ^{0.33})	-0.023	-0.029	-0.038	-0.034
±SD	0.0024	0.0035	0.0057	0.0044
COM y (/femur length)	-0.402	-0.532	-0.500	-0.466
±SD	0.043	0.072	0.077	0.059
COM y (/limb length)	-0.116	-0.156	-0.148	-0.132
±SD	0.012	0.019	0.023	0.016
COM y (/body length)	-0.080	-0.106	-0.111	-0.099
±SD	0.0084	0.016	0.018	0.013
Trunk COM y (/femur length)	-0.378	-0.524	-0.478	-0.446
±SD	0.040	0.066	0.071	0.067
COM z (/body mass ^{0.33})	-0.020	-0.019	-0.014	-0.022
±SD	0.0047	0.0046	0.0096	0.0089
COM z (/femur length)	-0.347	-0.350	-0.192	-0.292
±SD	0.091	0.075	0.13	0.12
COM z (/limb length)	-0.100	-0.103	-0.057	-0.083
±SD	0.025	0.023	0.038	0.035
COM z (/body length)	-0.068	-0.070	-0.042	-0.062
±SD	0.016	0.017	0.028	0.026
Trunk COM z (/femur length)	-0.354	-0.350	-0.192	-0.299
±SD	0.091	0.062	0.12	0.10

x, cranial; y, ventral; z, medial relative to right hip.

TABLE 4. Air space inflation sensitivity analysis for adult junglefowl cadaver

Model	COM cranial (x)	COM ventral (y)	Cranial diff (%)	Ventral diff (%)	Ratio cranial	Ratio ventral	Estimated/actual mass (%)
Lifelike, no cavities	0.086	-0.019	172	41	1.3	0.41	131
Minimal inflation	0.087	-0.023	174	50	1.4	0.49	118
Maximal inflation	0.092	-0.026	184	57	1.4	0.56	103
Straightened, detailed	0.064	-0.047	128	101	n/a	n/a	129
Straightened, no cavities	0.062	-0.042	124	91	0.97	0.90	148
Simplified, max caudal	0.044	-0.066	88	143	0.69	1.4	125
Simplified, max cranial	0.065	-0.041	130	89	1.0	0.88	150

COM positions are in meters. The “lifelike, no cavities” model was posed as in Fig. 5A,B. The “minimal” and “maximal” inflation models had air sacs deflated or inflated as described in the Methods; these were added as cavities to the lifelike model. All three of these models had body segment poses approximating those during standing (not recumbent as in scans from Table 3 or Fig. 2). The “straightened, detailed” model had its body segments straightened (Fig. 5C,D) but was based on the original scan geometry (detailed anatomy) and had internal “relaxed” cavities matching the original scans. The “straightened, no cavities” model simply lacked these cavities. The two “simplified” models used the basic skeletal geometry of the “straightened” model as an underlying framework around (or into) which deformable hoops representing flesh distribution (or cavities) were placed; the “max caudal” model had flesh distribution biasing the COM to a more caudal position (Fig. 5E), the “max cranial” model to a more cranial position (Fig. 5F; refer Methods). The “diff” columns (cranial and ventral) show the differences (ratio as a %; 100% = identical) of the cranial and ventral COM positions from the originally-scanned recumbent specimen (pose as in Fig. 2); x and y COM positions were 0.050 m and -0.046 m, respectively. The “ratio” columns give model values relative to the “straightened, detailed” model; 1 = identical. The “estimated/actual mass” column gives % difference from actual body mass of 2.069 kg; 100% = identical.

damaged condition of their presacral regions or limbs. We scanned (as above; 1.5 mm slice thickness, 2.13–2.56 pixels mm⁻¹) one adult green iguana (*Iguana iguana*), one adult savannah monitor (*Varanus exanthematicus*), and one subadult basilisk lizard (*Basiliscus vittatus*).

To assess the deviation of tail cross-sectional shapes from those suggested by the caudal skeleton, and their effects on inertial properties, we segmented the flesh and skeleton as separate 3D meshes in MIMICS. In Blender software, we then fitted simple octagonal hoops

TABLE 5. Tail deformation sensitivity analysis for crocodile cadavers

		"REAL" COM (m)				
Crocodile	Tail reconstruction	Cranial (x)	Ventral (y)	Medial (z)	Estimated/ actual mass (%)	
Juvenile	Standard				87	
Juvenile	Informed	0.047	-0.013	-0.021	99	
Adult	Standard				86	
Adult	Informed	0.119	-0.012	-0.053	99	

		Estimated COM x (m)			Estimated COM y (m)			Estimated COM z (m)		
Crocodile	Tail reconstruction	Max	Min	diff	Max	Min	diff	Max	Min	diff
Juvenile	Standard	0.100	0.073	0.040	-0.016	-0.013	-0.002	-0.022	-0.022	-0.001
Juvenile	Informed	0.084	0.034	0.012	-0.016	-0.013	-0.002	-0.022	-0.022	-0.001
Adult	Standard	0.213	0.142	0.059	-0.021	-0.010	-0.004	-0.058	-0.055	-0.004
Adult	Informed	0.182	0.066	0.005	-0.022	-0.014	-0.006	-0.056	-0.053	-0.002

COM positions are in meters. "Tail reconstructions" are: Standard = tail shape represented as simple ellipse; Informed = tail shape deformed from "hoop" method (Figs. 3, 6, and 7). "Real" COM is from straightened, detailed models in Fig. 1C,D, but with actual air spaces (from CT scans; as in Fig. 1E) included. The "estimated/actual mass" column gives % difference of mean model value [(max + min)/2 from below] from actual body masses in Table 1; 100% = identical. "Estimated" COM is for simplified models (e.g., Fig. 1F-H); "max" and "min" columns are for maximal (+20%) and minimal body outlines; "diff" column is mean model value [(max + min)/2] minus "real COM" from section earlier.

(Fig. 4) tightly to the caudal skeleton at regular intervals, again representing the fleshy outline suggested by assuming elliptical cross sections and using skeletal dimensions alone. These skeleton based outlines were then systematically deformed until they closely approximated the actual fleshy cross sections, varying mediolateral, dorsal, and ventral dimensions to account for size differences. To account for differences in outline shape, the dorsal and ventral diagonal dimensions (Fig. 4) of each octagonal hoop were each scaled (varying the basic ellipse-approximating shape to one closer to a diamond or a square) in a crude approximation of the superellipse approach described by Motani (2001). To represent typical saurian tail dimensions, we calculated a mean of these deformations for all specimens.

For one adult junglefowl cadaver, we conducted a sensitivity analysis of actual air space dimensions, to approximate the effects of ventilation (air space volume changes) on COM position, and to determine the effects of differing estimates of air space volume or even total exclusion of the air spaces on COM estimates. We suspended the specimen via threads from the pectoral and pelvic girdles to avoid deformation of the chest cavity by the cadaver's weight, and posed its body and limbs to match photographs of standing junglefowl (allowing a comparison with models that were posed in more recumbent positions). Air was then injected or removed from the pulmonary system using a large syringe barrel attached via a length of tubing inserted into the trachea. The plunger of the syringe was either depressed or extended until significant resistance was met, representing "maximal inflation" (addition of ~150 mL of air) and "minimal inflation" (i.e., deflation; removal of ~45 mL of air), respectively, and secured in this position while the specimen was CT-scanned. The resulting maximal and minimal pulmonary cavities were segmented as 3D shapes in MIMICS (Fig. 5A,B), and modeled for inertial

properties in our custom software as above (setting cavity densities as zero).

We used SPSS 15.0 (Statistical Package for the Social Sciences, Chicago, IL) software for statistical analysis, to check for differences of COM estimates between chicken cohorts. One way analysis of variance (ANOVA) was used to test the differences among several means with the cohort as the factor and the COM value as the dependent variable. If a significant result was shown, a sequential Bonferroni *post hoc* test was used to establish which cohorts were significantly different. An adjusted *P*-value < 0.05 was considered statistically significant. A *t*-test was used to examine the effect of MIMICS segmentation and the COM estimation procedure for differences between the two groups.

RESULTS

Detailed results for our models are presented in the Appendices (Tables A1-A5), but we summarize our key findings here.

Estimated Versus Actual Body Mass and Density

In crocodiles (Table 1), our model of the juvenile overestimated actual cadaver body mass by 16%, whereas the adult model overestimated mass by 5%. These data indicate a slightly higher density (948 kg m⁻³) for the adult versus the juvenile (860 kg m⁻³). Curiously, the adult's density is only 88% of the 1080 kg m⁻³ estimated by Cott (1961). Predominance of low-density cartilage and other tissues in juveniles, especially for the armored scutes, may explain the apparent ontogenetic difference in density, supported by our dissections and examinations of the CT scans. COM values in the initial models with density equal to water (Table 2) are biased

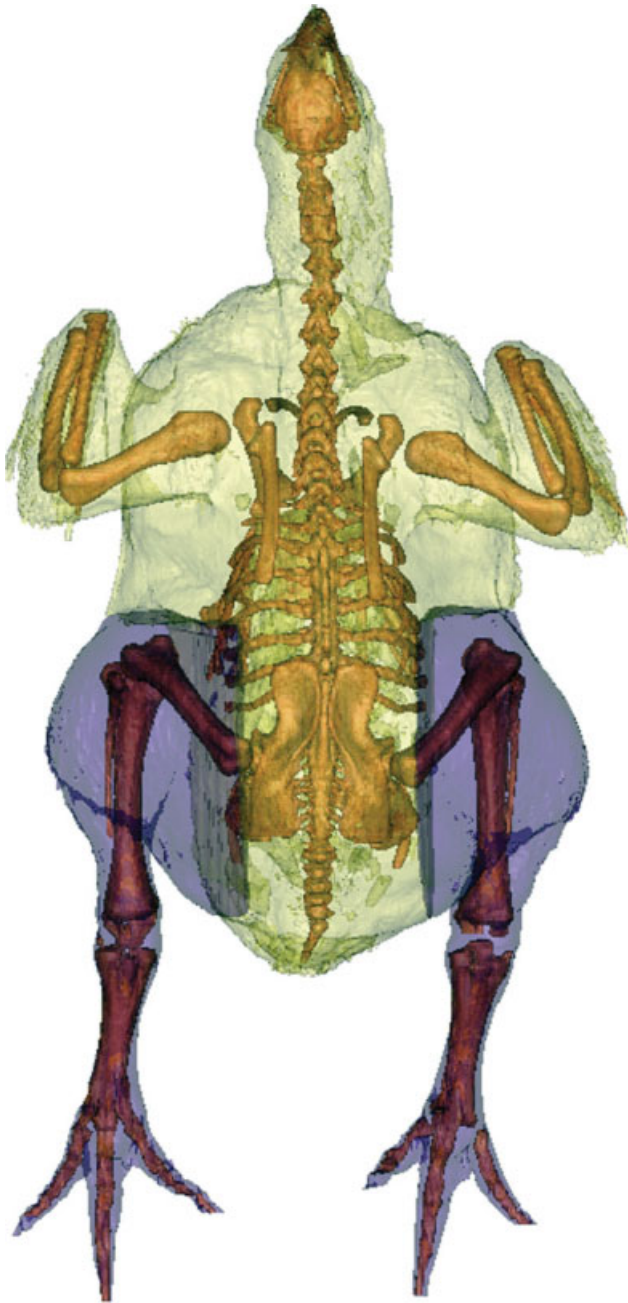


Fig. 3. Procedure for digitally removing chicken limbs to estimate the trunk center of mass (refer Methods and Table 3 for further details). A “mature” broiler chicken is shown in dorsal view (yellow = trunk; purple = removed pelvic limbs), with flesh translucent and skeleton (for reference) more opaque. Not to scale.

accordingly. We address this point further below by examining effects on COM by including realistic air spaces in the crocodile models.

We also assessed the effects on body mass estimates from assuming a homogeneous 1000 kg m^{-3} density for the birds, finding that our method uniformly overestimated the actual masses by only 3%–5% for broiler chickens and 10%–12% for junglefowl (Table 1), worsen-

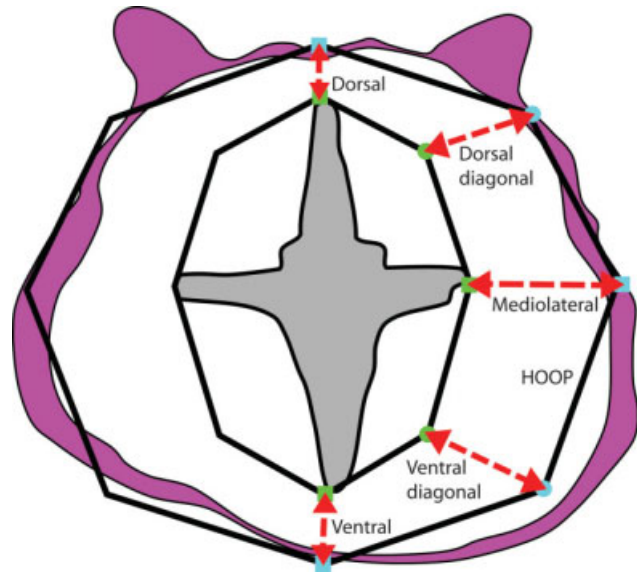


Fig. 4. Tail deformation method to examine the extents of body outline beyond skeletal landmarks, shown for a proximal cross-section of a juvenile *Crocodylus* tail. An initial octagonal hoop (inner one) is fitted to the neural spine, transverse processes and chevron (gray interior shape; green points). The hoop is then scaled (red arrows, from green points to blue points on outer hoop) to approximate the fleshy outline (magenta irregular shape) as a larger outer hoop (labeled “HOOP”). The required deformations from smaller (skeletal) to larger (fleshy) hoops are thus recorded (e.g., $1.7 \times$ mediolateral deformation shown). Not to scale.

ing with growth. Thus, the actual mean densities of the birds were closer to 950 and 900 kg m^{-3} ; unlike in the crocodiles there was no appreciable change of mean density across the two ontogenetic series. Again, as COM positions may be affected by our omission of air spaces in these models, we examine the influence of cavity volumes on COM positions further below.

Variation Within Chicken Cohorts

Body mass estimates varied similarly to or slightly higher than actual body masses (SD values in Table 1). Estimated COM positions varied appreciably within each group of chickens examined (Table 3). Standard deviations were moderately high in some cases, presumably due to the low sample sizes (5–10) and variable limb/body poses during CT scanning (Fig. 2). In the medial (z) direction, this variation was relatively the highest (standard deviations averaging 35% of the mean values), followed by cranial (x) at 14% and ventral (y) at 13% standard deviations/mean value. In all cases, the method we used to normalize these COM data for comparison had negligible effects on this variation.

Variation Between Chicken Cohorts

The moderate COM variation within our cohort samples complicated statistical analysis of differences between them (Table 3), but nonetheless the juvenile junglefowl had significantly more caudally positioned whole body COMs (mean 38% femur length cranial to the right hip) compared with the other cohorts (mean

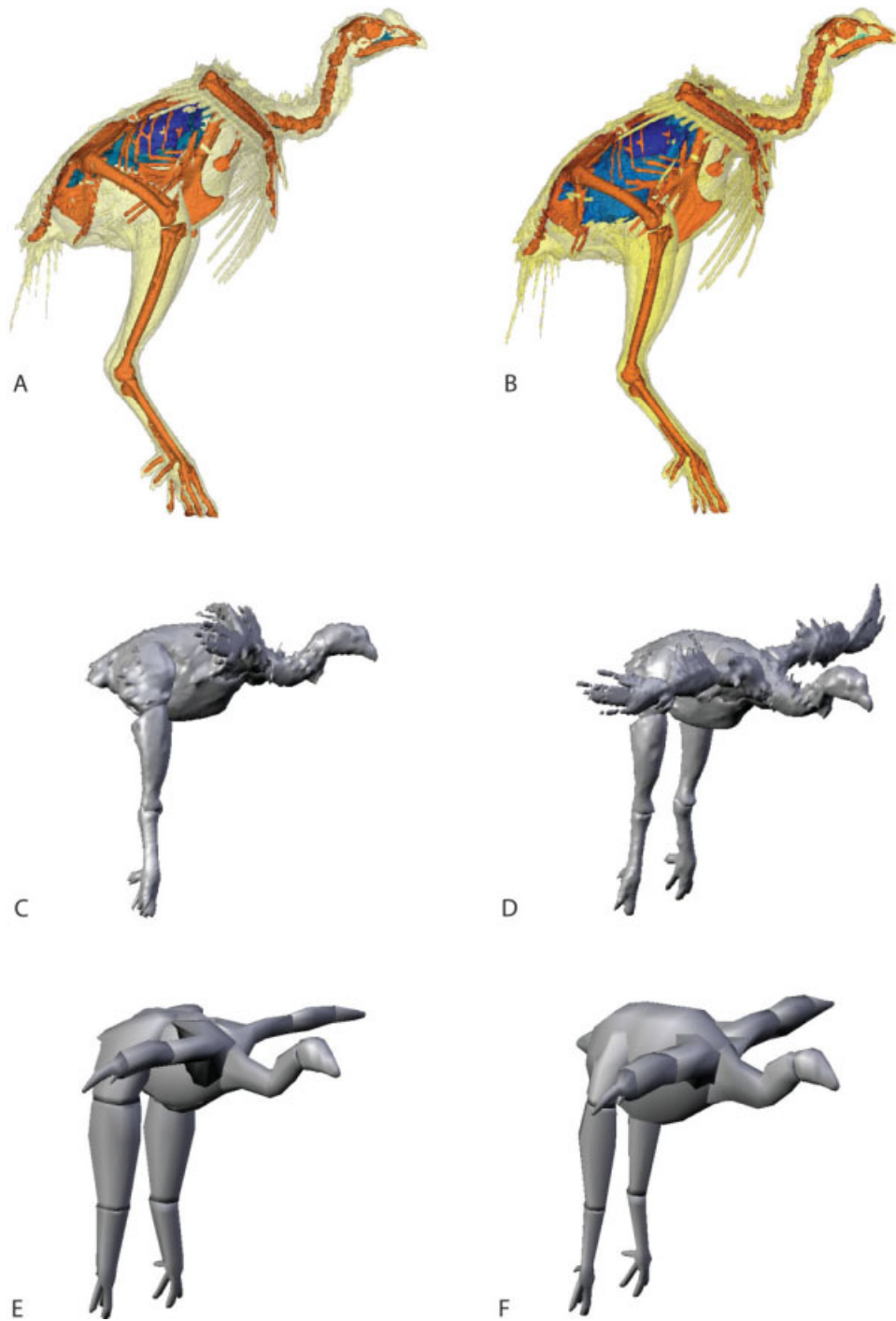


Fig. 5. Junglefowl inflation method to examine the effects of air space geometry on center of mass positions for Table 4. **A,B:** Right lateral views of adult junglefowl model in “lifelike” pose with minimally (A) and maximally (B) inflated air spaces. Blue interior objects represent the air spaces. The flesh and feathers are rendered transparent (in yellow) and the skeleton is opaque (in orange; for reference only, not used for estimating inertial properties). **C,D:** Right lateral and right oblique views of “straightened, detailed” model of same specimen,

showing how limbs were extended into the reference pose. **E,F:** Right oblique views of “max caudal” (E) and “max cranial” (F) simplified models (using the octagonal hoop deformation method as in Fig. 1E), showing how body shape was deformed by biasing mass distribution caudally/cranially (refer Methods), to bound ranges of inertial property values (Table 4). Not to scale; scaled to same total length in each pair of images.

54% femur length cranial to the right hip). Additionally, the juvenile broilers had significantly more dorsal whole body COM positions (mean 40% femur length) except compared with adult junglefowl (mean 47% femur length). The other cohorts had a collective mean of 52% femur length and neither one was statistically similar to the former two or different from each other. There were no observed significant differences between mediolateral whole body COM positions of any cohorts. Any actual significance may have been obscured by the variation noted earlier.

Ontogenetic Variation

The models of juvenile and adult crocodiles (Table 2) suggest that the COM shifts craniodorsally (when expressed in terms of femur lengths) across ontogeny in *C. johnstoni*. The shift was most striking in the cranial direction, changing from 92% to 120% femur lengths (+28%) with a 1,189% change of body mass. The changes of COM position dorsally and medially were smaller (~10% of femur length). Substantial error was introduced by the more abducted (dorsal) posture of the limbs when scanned (Fig. 1A,B). Table 2 shows that the originally scanned pose had COM positions that were 52%–167% of the straightened reference pose COMs. In addition, the relatively shorter femur in the adult complicates the usage of femur length for normalizing COM positions. Nonetheless, the observed ontogenetic differences between the original and straightened models are preserved when trunk (body *sans* limbs) COM values are compared as well (Table 2). Therefore, the major ontogenetic changes of COM are caused less by limb dimensions or positions than by trunk shape.

For the birds (Table 3), the broiler chickens exhibited a caudoventral shift of the whole body COM from juvenile to mature individuals, but interestingly the junglefowl showed an opposite shift: craniodorsally from juvenile to adult. As earlier, other errors in the analysis such as body segment orientation during scanning and body proportions may cause inaccuracies in our quantitative estimates; we examine these further below.

Variation Due to Methodology

Human error in estimating whole body COM positions was assessed by resegmenting and re-estimating body mass and COM values for the same five mature broiler chickens, starting from the same raw CT scan data. The same operator did all of these procedures. Repeated estimates of body mass were underestimated by a mean of -0.099 kg from original values (range, -0.005 to -0.266 ; SD 0.105 kg) or on average only 2.9% of body mass. Estimated COM positions were 46 ± 7.1 , 53 ± 5.6 , and 40 ± 5.0 percent of femur length in the cranial, ventral, and medial directions (mean \pm SD) for this second measurement, compared with 50 ± 8.6 , 53 ± 7.2 , and 35 ± 7.5 percent femur length for the first measurements (Table 3). Repeated measures *P* values for these COM positions were 0.420, 0.909, and 0.254, respectively, so this variation was not significant.

Increasing resolution (reducing slice thickness) for representative mature broiler chicken and adult junglefowl models had small effects on body mass and whole body COM values. After repositioning the specimen and

scanning at higher resolution, body mass was overestimated by 0.090 kg (+3.3% cf. with the first scan, which itself overestimated the real body mass by 2.9%). The broiler COM values were 8% more medial, 5% more ventral, and only 83% as cranial (percentages relative to femur length) as in the lower-resolution scan. Without specimen repositioning, at higher resolution the junglefowl specimen mass was again overestimated by 0.133 kg (+7.1% cf. with the first scan, which itself overestimated the real body mass by 7.9%). However, its COM values (normalized by femur length) as expected fared better than for the broiler: 93% as medial and ventral, and 100% as cranial as in the lower-resolution scan. Overall, variation due to scan resolution appeared considerably smaller than errors introduced by segmenting the CT scan data or especially repositioning the specimen.

As noted earlier, specimen pose also had large effects on crocodylian COM estimates medially and especially cranially (Table 2)—overestimating cranial COM position by 33% (1.6/1.2 femur lengths) in the adult, and underestimating it by 60% (0.55/0.92 femur lengths) in the juvenile crocodile. Dorsoventral COM position was unaffected.

We found that it did not matter which frame of reference (normalized by body mass^{0.33}, femur length, pelvic limb length, or body length) was used for the chicken models; the same statistically significant differences noted above were found for all four normalization methods (Table 3). We also found that acetabular position as a percentage of body length was consistent (and statistically identical; ANOVA: $F = 2.161$, $P = 0.133$) among all cohorts (mean $80 \pm 1.5\%$ SD), so using the right pelvic joint as a reference point for all COM normalization methods involves an assumption (constant relative position of the right acetabulum) validated here.

Digital removal of the pelvic limbs to estimate trunk (body *sans* hindlimbs and associated muscles) COM positions for chickens showed interesting differences from the analyses focusing on whole body COMs (Table 3). Statistically significant differences were found along the craniocaudal axis (juvenile broiler COMs were positioned more cranially than in mature broilers: mean 93% vs. 83% femur length; other cohorts were intermediate between these values but not statistically different from either). Trunk COM ontogenetic shifts thus matched those inferred for the whole body COMs (above; same as for the crocodiles in Table 2). No statistically significant dorsoventral differences were found. Mediolateral COM positions were significantly different between juvenile broilers and juvenile junglefowl (38% vs. 48% femur length; broiler trunk COMs apparently more medial because their pelvic widths are larger, moving the acetabular reference point laterally).

Variation Due to Air Space Geometry and Other Factors

Body masses for the inflated junglefowl model improved their match to the actual measured mass of the cadaver with increasing air space inflation (Table 4), from a 31% overestimate without air spaces (for this specimen, higher than the 12% average error in Table 1 for other individuals), to only a 3% overestimate with maximal inflation. Note that body shape did not change

with inflation in our models; only air space volume was changed, which explains why estimated mass decreased. The 31% mass estimate error raises concern for accurately estimating masses of extinct animals and using those estimates in higher-level inferences such as locomotion or metabolism. This concern is reinforced by other models with straightened limbs and varied body shapes; 29%–50% mass estimation errors are common (Table 4). The best match with the actual body mass was obtained using the “maximal inflation” model (3% overestimate).

While our comparisons show that we overestimated mass and density for the specimens studied (Table 1; also see earlier), how much do air space dimensions alter the COM positions? For a junglefowl with air spaces ranging from absent to deflated and maximally inflated, posed in a “lifelike” body segment orientation (Fig. 5A,B), we found that the COM shifts cranioventrally with larger air spaces, and the effects of air space geometry are generally larger in the ventral direction than cranially in chickens.

Yet how much of these differences were due to different body segment positions rather than air space dimensions? To investigate this, we first reposed the model into a “straightened, detailed” version including “relaxed” air spaces (Table 4, fourth model; Fig. 5C,D) that was in a vertically legged reference pose (refer Methods). We then also removed the cavities from this model. In the latter model, the COM moved only 4% caudally and 10% dorsally, showing that the cavities alone have small effects on COM positions. In contrast, the alterations of body pose between the straightened model and the original, recumbently posed model (Fig. 2) had almost an order of magnitude greater influence on body COMs than cavities did (“diff” column in Table 4). These differences ranged from 172% to 184% as cranial and 41% to 57% as dorsal (in absolute values) compared with the original recumbent scanned pose (Table 3), versus 128% and 101% as cranial and dorsal for the “straightened, detailed” model versus the original recumbent pose. Thus, body segment orientation alone can cause ~50%–80% differences in the chicken COM positions, and accounts for most of the COM differences in Table 4. However, there seemed to be a tradeoff between accurately estimating mass and COM. The “straightened, detailed” model overestimated mass by 29%, or 48% without cavities, which accounts for most of the mass estimation differences in Table 4.

This variance can be greater than the effects of representing the real, detailed anatomy by simple (but plausible) geometry. This step approximates the errors imposed by an unknown relationship of fleshy to skeletal dimensions that confounds mass and COM estimates for extinct taxa (refer Methods). Compared to the “straightened, detailed” model (Fig. 5C,D), simplified models with extreme body dimensions that were biased toward caudal (Fig. 5E) or cranial (Fig. 5F) COM positions introduced differences in COM positions that ranged from –31 to +40% (“ratio” column in Table 4). Thus, the step of moving from an anatomically realistic model to a simplified representation, even in the best cases where anatomy is well known, can have more influence (<40%) on COM positions than the effects of air space geometry (<10%), but sometimes less influence than body segment orientations (~50%–80%). Mass estimation errors were

comparable to the other models; 25%–50%. Again there was a tradeoff—simplified models that matched the “straightened, detailed” model COM values more closely matched the actual mass less closely.

Tail Profile

We found that saurian tails had fairly conservative geometric outlines relative to the underlying skeleton, even across amphibious and highly terrestrial species (iguanaid and varanid lizards, and crocodiles), shown in Figs. 6 and 7. All fleshy outlines were found to be substantially larger than those suggested by the skeletons (typically 140%–200%). Along the mediolateral and ventral axes, the deformations of the initial skeletal outlines (Fig. 4) required to match the sizes of the actual fleshy dimensions had the largest mean magnitudes (158% and 186%, excluding data mentioned below for caudal three ventrally and caudal 14–15 mediolaterally) and variability (SD values 28%–30% of the means). The dorsal deformations required to fit the actual dimensions were smaller (mean 133% deformation). Alterations to general outline shape, controlled by scaling the diagonals, were generally of smaller magnitudes and less variability than those required for size (91% dorsal diagonals, 112% ventral diagonals; SD values 8%–16% of the means), indicating that saurian tails have a conserved “teardrop”-shaped cross-section. We also examined the chicken tails but these simply followed the general body contours so they were problematic to compare with non-avian tails using our method.

Juvenile and adult crocodiles displayed a consistent pattern of extra skeletal tail dimensions (Fig. 7), differing from those seen in lizards mainly in the substantial deformations required at the mid tail (350%–400%, peaking at caudal vertebra 14–15 and more pronounced in the adult). This region is the transition point, where the transverse processes (and hence mediolateral skeletal dimensions) are strongly reduced but the tail musculature (and hence mediolateral body dimensions) is not. For crocodylians this suggests that the transverse processes are poor indicators of tail width around the transition point. However, in the lizards extra skeletal dimensions were remarkably consistent throughout the tail (Figs. 6 and 7), except in the proximal tail where chevrons were absent. In that region, as would be expected, the deformations required were much larger and more variable in lizards (Fig. 6A, caudal vertebra three ventral deformation of 600% in *Iguana*; also 1,600% in *Varanus*; 360% in *Basiliscus*; not shown). This is because, in the absence of chevrons (hemal arches), the ventral extent of the skeleton is defined by the centra, and the proximal tail musculature extends far below this point. This effect was less prominent in the two crocodiles, which had proximal tail chevrons. Although this represents a real issue—in at least some lizards there are no adequate skeletal landmarks in the proximal tail that predict its ventral extent—we removed these very high outlying values for the proximal tail to improve the results of our calculations of average caudal extra skeletal dimensions. This assumption will remain the most valid for taxa with proximal caudal chevrons, as in many dinosaurs.

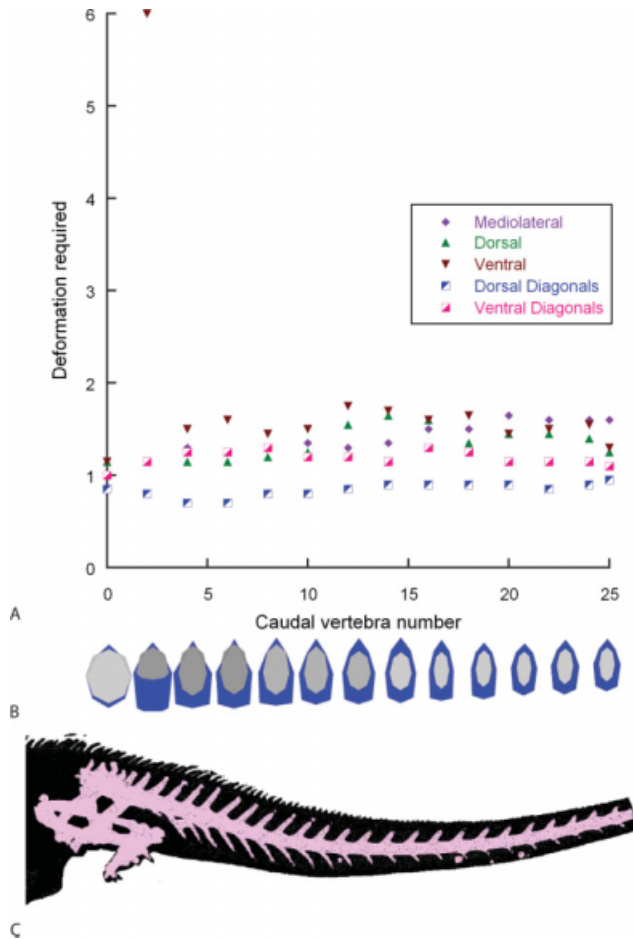


Fig. 6. Tail deformation results for a representative saurian tail (adult *Iguana iguana*). **A**, Graph of deformation required along axes shown in Fig. 4, versus caudal vertebra number (plotted for every even-numbered caudal vertebra segment). **B**, Approximate shapes of octagonal hoops to represent the caudal skeleton (light gray) and deformed octagonal hoops to represent the extra skeletal body outline (dark blue) corresponding to positions along the x-axis in **A**. **C**, Segmented CT scan data for the same specimen (in left lateral view), oriented to roughly match **A** and **B**; flesh in black and skeleton in pink. Not to scale. Data terminate where the plot reaches a plateau that continues to the distal end of the tail; for simplicity the entire tail is not shown.

Effects of Tail Dimensions on Inertial Properties

We compared our best crocodylian models, with the most realistic body (including tail) outlines and internal air space anatomy (Table 5: “real” COM columns; Fig. 1C,D; air spaces in E), to simpler estimation procedures (Table 5: bottom section; Fig. 1F–H). These simpler models began with skeletal anatomy alone (Fig. 1F) and reconstructed surrounding soft tissues simply from these landmarks (as for the junglefowl in Table 4 and Fig. 5). Two sets of maximal and minimal volumetric models of each crocodile were created. The first set used standard assumptions to recreate the tail (Fig. 4; elliptical cross sections fitted to skeletal dimensions for minimal volume, then plus 20% for maximal volume). The second set used the mean values (for the non-avian saurians, excluding artefacts noted earlier: 158%

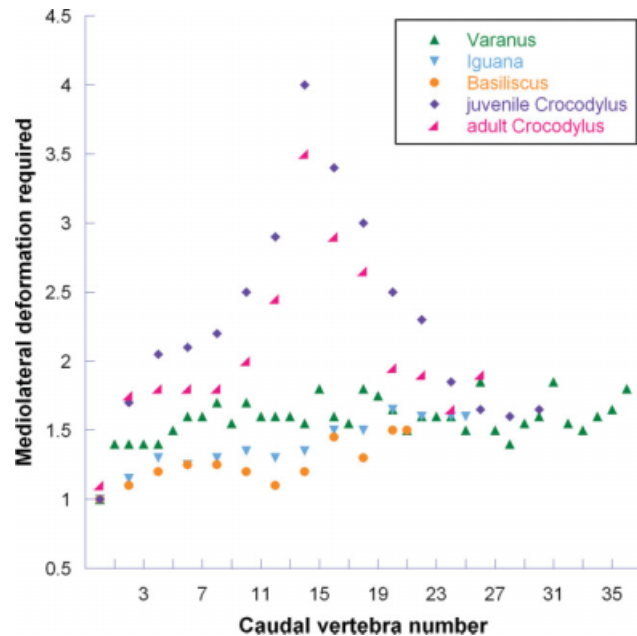


Fig. 7. Tail profiles for all five non-avian saurian taxa examined. Graph of octagonal “hoop” deformations required, starting from skeletal shape alone, along the mediolateral axis (as in Figs. 4 and 6) to match the body outline (y-axis), plotted against caudal vertebra number (x-axis; for every caudal segment). Note the increase of deformations required at the transition point (~caudal 15) in the crocodiles. Data terminate where the plot reaches a plateau that continues to the distal end of the tail; for simplicity the entire tail is not shown. These results imply that non-avian saurian tail shapes are fairly conservative, which can be used to inform estimates of tail shape and inertial properties in extinct saurians.

mediolaterally, 133% dorsally, 186% ventrally, 91% dorsal diagonally, and 112% ventral diagonally) for extra skeletal size and shape calculated from extant tail profiles (Figs. 4, 6, and 7), $\pm 20\%$ for maximal and minimal volumes.

The most detailed and realistic “informed” models closely approximated body mass (only 1% underestimate), whereas the “standard” elliptical tail models underestimated mass by 13%–14%. The informed models thus were a substantial improvement over the 5%–16% initial mass overestimates (Table 1), whereas the standard models changed the error to an underestimate but did not greatly reduce its magnitude.

Our COM estimates fared relatively worse in the standard versus informed tail models. In the juvenile crocodile, the standard model positioned the body COM a mean of 4 cm too far cranially (an error of 85%), which improved to 1.2 cm too far cranially (26% overestimate) with the informed model. The adult crocodile models improved even more substantially, from mean cranial overestimates of 5.9 cm (50%) to 0.5 cm (4%). For both specimens, ventral and medial COM estimates changed only trivially if at all (Table 5). Taking the mean of “minimal” and “maximal” models seemed to give the closest overall match to the “real” COMs, especially cranially. Overall, we found that assumptions about tail shape alone can cause large (here 50%–85%) errors that can be improved considerably (here reduced to 4%–26%) with our “informed” tail deformation method that takes into account typical saurian tail dimensions.

DISCUSSION

How Much Biological Variation of COM Values is Expected?

With our method, COM variation within chicken cohorts was moderately high (~35%) along the mediolateral axis and smaller (13%–14%) along other axes. We judge this variation to be largely due to variability of limb/body orientation during scanning (Figs. 2 and 5; Table 4) rather than intrapopulational variation, which is difficult to measure without larger sample sizes and highly consistent methods of measuring COM. Overall, the poses we used were adequate and allowed for fundamental differences between cohorts to be found. Broilers have more dorsal and cranial COM positions than junglefowl, which we ascribe mainly to their shorter, lighter pelvic limbs and larger pectoral muscles (pers. obs.). The more cranial COM positions would require more crouched limb poses and potentially increased joint and muscle moments, which deserve deeper investigation in light of domestic chicken health and welfare. In contrast, the more caudal COM position in junglefowl helps to maintain their proficiency in bipedal running (Hutchinson, 2004; Clemente et al., 2008). How the differences in dorsoventral COM position factor into this or the relative inclination of the main body axis (Hutchinson et al., 2007) remains to be seen.

Although we found that any frame of reference for normalizing COM values gives similar results, using trunk COM removes some of these problems of postural variation and reinforces the validity of the whole body COM differences found (Tables 2 and 3). However, our chicken cohorts had similar gross body morphology, and thus it may not be surprising that all normalizing methods gave similar results. For studies involving taxa of widely different body shapes, such as large dinosaurian clades, we urge that multiple normalizing methods be applied. Perceived differences or similarities of COM values among taxa may be due to independent variation of the normalizing factors used (e.g., allometry of body or femur length with body size) or the reference point used to express COM location (e.g., shifts of the acetabular position along the body axis). For example, our junglefowl “straightened, detailed” model (Table 4) has a cranial body COM position relative to femur length (0.74) over half that of the juvenile (0.92) and adult (1.2) crocodile models (Table 2). Yet usage of trunk COM gives quite different results (0.54, 1.6, and 1.94 femur lengths, respectively), as does usage of the “lifelike” (Fig. 5A,B; Table 4) pose for the junglefowl (1.0 femur lengths).

Similarly, the large ontogenetic change of COM positions inferred for *Crocodylus* partly depends on our usage of femur lengths to normalize them, although our findings still have relevance for understanding ecological shifts in crocodylians. The relative reduction of the limbs and relative craniodorsal shift of COM during ontogeny inferred probably applies to most crocodylians, judging from morphometric data (e.g., Dodson, 1975; Webb and Messell, 1978). This change, along with body density increases, should cause relative increases of loading on pelvic limb joints and muscles (Hutchinson, 2004), and thus could help to explain the decline of bounding (and galloping) capacity with increasing size in crocodylians (e.g., Cott, 1961; Zug, 1974). Similar ontogenetic shifts of COM influencing locomotor mechanics have been

inferred for other dinosaurs, such as the small ornithischian *Dryosaurus* (Heinrich et al., 1993) and the early sauropodomorph *Massospondylus* (Reisz et al., 2005).

Likewise, the ontogenetic changes in chicken COMs we found vary among cohorts—broiler chicken COMs shift caudodorsally, whereas Manion (1984) found that in white leghorn domestic chickens the COM shifts cranioventrally. Although on phylogenetic grounds it is tempting to infer that the craniodorsal COM shift in both *Crocodylus* and junglefowl is a shared archosaurian characteristic (archosaurian limbs often get relatively shorter while heads get more robust during growth, e.g., Bybee et al., 2006; this should draw the COM craniodorsally), this demands broader taxonomic investigation. This caution is reinforced by the wide phylogenetic distance between the two extant clades, the small sample sizes (especially for crocodiles), and the considerable variation in domestic chickens despite only moderate evolutionary morphological changes, compared with drastic morphological changes in extinct dinosaurs.

How Much Methodological Error for Mass and COM is Expected?

We have found that anatomically accurate models can estimate body mass with a reasonable margin of error (e.g., 1% under- to 16% overestimate for crocodiles, with chickens falling inside this range). This error is largely, as expected, due to inappropriate assumptions about density, including air spaces (especially for birds), as well as ontogenetic changes and tail shape (especially for crocodiles). However, these density effects are generally stronger on body mass than on COM positions. As most air spaces, especially the lungs, lie close to the COM, air space geometry has little effect on COM values (e.g., Table 4; also Henderson, 2003; Hutchinson et al., 2007; Bates et al., 2009). We found body mass estimates nonetheless to be repeatable (~3% variation). Judging from similar variation found for different CT resolution settings, this variation is probably largely due to human error in segmenting CT scan data rather than poor image resolution of anatomy.

The main concern for estimations of body mass in extinct taxa, however, is properly estimating body density (~10%–15% source of error). If juvenile crocodiles and adult birds are a reliable guide (Table 1), mean densities of ~860–894 kg m⁻³ are good starting assumptions (although it is surprising that juvenile crocodiles can be less dense than chickens). That density range compares favorably to values for an ostrich carcass (888 kg m⁻³) and ranges of estimates for models of *Tyrannosaurus* (787–894 kg m⁻³) from Hutchinson et al. (2007). “Best estimates” by Bates et al. (2009; Tables 1–6) for a whole ostrich were similar (857 kg m⁻³), but curiously averaged slightly higher for various dinosaurs, around 900–940 kg m⁻³ (sensitivity analysis in their Table 7: 866–947 kg m⁻³).

Density estimates might be improved by carefully modeling detailed air space anatomy and entering specific values for tissue densities within segments (e.g., fat, muscle, bone, cartilage). Yet we see this as certain to introduce more assumptions (each of which must be varied for extinct taxa) but not certain to appreciably constrain the probable density range. Hence it would quickly become more of a technical distraction than a

TABLE 6. Center of mass methods applied to *Tyrannosaurus rex*

<i>T. rex</i> model	COM (m)				COM (femur lengths)					
	COM cranial (x)	COM ventral (y)	Cranial diff (%)	ventral diff (%)	COM cranial (x)	COM ventral (y)	Cranial diff (%)	Ventral diff (%)	Body mass (kg)	Mass diff (%)
Original (#1)	0.599	-0.289	115	104	0.49	-0.24	115	104	5450	83
Best guess (#30)	0.519	-0.279	100	100	0.43	-0.23	100	100	6583	100
Max cranial	0.785	-0.283	151	101	0.64	-0.23	151	101	8205	125
Max caudal	0.133	-0.344	26	123	0.11	-0.28	26	123	6773	103
Max dorsal	0.524	-0.258	101	92	0.43	-0.21	101	92	8973	136
Max ventral	0.424	-0.324	82	116	0.35	-0.27	82	116	6009	91
Mean	0.459	-0.291	88	104	0.38	-0.24	88	104	7593	115

Original (#1; minimally “skinny” model) and “best guess” (#30; tail enlarged 21%, rest of body 10%) models are from Hutchinson et al. (2007). The remaining models used the skeletal landmarks from that study and the octagonal hoop deformation method and “informed” tail shape (as in Table 5; also Figs. 4, 6, 7 and refer Methods) from this study. Differences (“diff” columns) between the best guess model and all other models are shown for absolute and normalized COM positions, and for body mass; 100% = identical values.

rigorous methodological improvement. Considering the small effects of density on COM values, we see little value in pursuing that approach, easy as it would be to do so with modern imaging technology (e.g., Mungiole and Martin, 1990; Wei and Jensen, 1995; Wicke et al., 2008).

We have shown that computational methods for estimating COM positions are fairly repeatable and with sufficient geometric resolution can give reliable results (within ~5%–8% total variation). These errors are additive to the errors noted above for limb and body (including head/neck) orientation, which we urge must be standardized carefully in any comparative studies of COM—an important omission from previous studies such as Bates et al. (2009). This point is demonstrated by our models of recumbent (Fig. 2, Table 3) versus more upright (approximating standing; Fig. 5, Table 4) junglefowl. With these changes of limb (and head/neck) orientation alone, COM values shifted cranially +28%–72%, and ventrally -59% to dorsally +1% (Table 4: “diff” columns).

As almost all methods for estimating COM even for extant taxa involve some error in image resolution, repeatability and body segment orientation, we caution that ~10%–15% error in COM estimates is a “best case” scenario for most methods. Some errors in our COM estimates, using an approach identical to that used to estimate COM for extinct taxa, even approached or exceeded 50% (Tables 4 and 5). Even force platform measurement of COM during standing *in vivo*, which might be the “gold standard” approach, involves photogrammetric errors and individual variation (in standing limb poses) that are likely to be of similar 10%–15% total magnitudes.

Where known experimental values have been compared with modeling/regression estimates for the same subjects in other studies, COM values, like masses, generally have been accurately estimated (within ~10%). In contrast, 10%–40% errors in inertia values are not uncommon (Hatze, 1980; van den Bogert et al., 1989; Sarfaty and Ladin, 1993; Baca, 1996; Norton et al., 2002), and 20%–80% errors are common when estimating inertial properties for individual subjects from group regressions (e.g., Challis, 1999). The influences of errors in COM and other inertial properties on biomechanical

analyses vary widely (Jensen, 1989; Krabbe et al., 1997; Pearsall and Costigan, 1999; Dellanini et al., 2003; Rao et al., 2006; Reinbolt et al., 2007), but naturally are greatest for larger, more proximal segments. Thus all studies using COM values as input properties should minimally consider 10%, and for extinct animals ~50%, potential total error (e.g., Hutchinson et al., 2007).

Tail Dimensions as a Major Component of COM Error

Structures most cranial and caudal to the body COM will influence its position the most. Head dimensions, however, can be well-constrained by skull geometry (pers. obs., this study and Hutchinson et al., 2007), and the head is generally lower in density and mass than the tail (except in crown group birds and their relatives). As Motani (2001) suggested, assumptions about tail shape can greatly influence COM (and other inertial property) values, biasing them toward inaccurate cranial values. We found that indeed non-avian saurian tails deviated appreciably (90% to >>200%) from elliptical shapes suggested by skeletal landmarks, and had major effects on COM estimates (Table 5). We therefore suggest that, for non-avian saurian taxa with unreduced tails, including extinct dinosaurs, these mean values for tail deformations are a good initial assumption grounded in phylogenetic optimization and quantitative empirical data, and should lead to considerably improved estimates of body or tail segment mass and particularly COM. To test the effects of this procedure, we next try this method on a well-studied dinosaur, *Tyrannosaurus*.

Estimation of Inertial Properties for an Extinct Dinosaur

Finally, we test our revised understanding of factors influencing the accuracy of inertial property estimation by revisiting the estimated mass and COM of an adult *Tyrannosaurus rex* (Dinosauria: Theropoda), as in Hutchinson et al. (2007). We applied the same octagonal hoop-based body shape estimation as in Table 5, including the “informed” tail shape, and air space geometry (also Figs. 1F–H, 4, 6, and 7). Table 6 shows the results for different models with extreme cranial, caudal, dorsal,

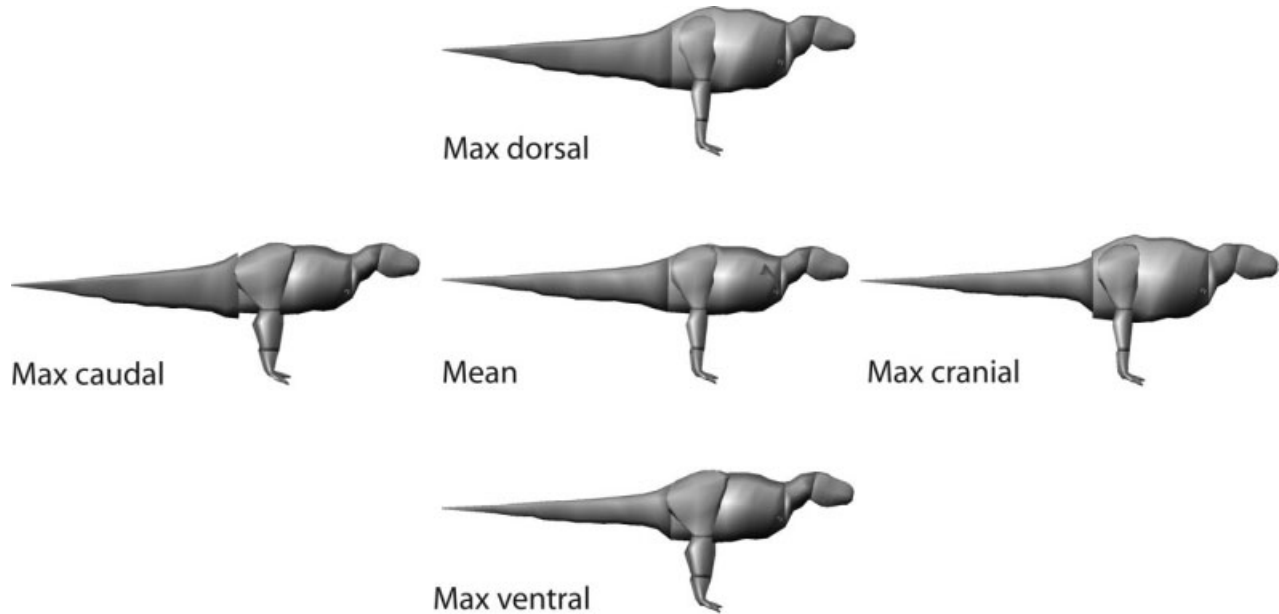


Fig. 8. Revised models of *Tyrannosaurus rex* following the methods developed here to estimate the inertial properties (Table 6), and using the skeletal dimensions from Hutchinson et al. (2007) from which to deform overlaid octagonal hoops that represent fleshy body outlines. Center: mean model with only moderate deformations. Maximal dorsal

and ventral COM positions induced by 20% deformations beyond the initial shape are above and below, respectively, and maximal cranial and caudal COM positions are left and right, respectively. Not to scale; scaled to same total length.

and ventral mass distributions, and Fig. 8 shows the five resulting models. The mean of these improved models compares favorably in COM positions with the “best guess” improved model of Hutchinson et al. (2007; 88% as cranial and 104% as ventral), but with a 15% larger body mass. It is further from the values for the original “skinny” model, which had a tail shape based upon a standard elliptical cross-section.

These revised models support the inference that the COM of *Tyrannosaurus* was further caudally positioned and it had a slightly larger body mass (>6,500 kg or even >8,000 kg) than previously assumed. Application of the methods suggested here to other dinosaur models (e.g., Bates et al., 2009) should have similar effects. As Motani (2001) cautioned, unsupported assumptions about tail and other body segment shapes are a major cause of these errors. However, as these estimates generally lie within the bounds of those considered by Hutchinson et al. (2007) they do not appreciably alter their conclusions about turning or running mechanics, but do refine them.

CONCLUSIONS

To date, studies estimating COM (and body mass) for extinct animals have only been weakly validated by applying the same techniques to living animals (often with no knowledge of actual masses or COMs for individuals) and examining the individual variation/error sources introduced. Our analysis of these factors identifies the major problems in, and provides decent validation for, computational techniques for estimating inertial properties. Expected variation and errors of at least 10%–15% for mass and 10%–50% for COM should be examined; inertia values depend on these and other fac-

tors, and are thus anticipated to have slightly higher variation. An error of 10% in a best case situation probably poses minimal problems for modeling locomotor biomechanics, for example in extant taxa, so this method is well-validated for these applications where body dimensions can be obtained directly from scans of cadavers. We have suggested density values and a simple “octagonal hoop”-based deformation method that improves estimates of body segment dimensions, especially for the tail, that can be used in computational models of extant and extinct archosaurs. However, ontogenetic stages, body segment orientations, and frames of reference to normalize COM values for comparisons need cautious methodological control for all studies. Thoroughly considering these factors can potentially minimize errors and lead to better-constrained paleobiological conclusions.

ACKNOWLEDGEMENTS

The authors thank the BBSRC for grants BB/C516844/1 and BB/F01169/1 to J.R.H that enabled this research. They also thank the Department of Veterinary Basic Sciences at The Royal Veterinary College for support. Vivian Allen’s research was partly supported by a Sam and Doris Welles award from the University of California, Museum of Paleontology. Heather Paxton’s research was supported by a CASE Industrial Studentship from the BBSRC, sponsored by Cobb-Vantress Inc. They appreciate the influence of fellow members of the Structure and Motion Laboratory, Stanford University’s Neuromuscular Biomechanics Laboratory, and Padian Lab at the University of California. Martin Bäker, Sandra Corr, Peter Dodson, Alexis Wiktorowicz Conroy, and two anonymous reviewers are thanked for their

constructive feedback on earlier drafts of this manuscript. Allan Ball and Roy Mutimer are thanked for access to Cobb 500 broiler chickens, and Nick Anthony is heartily thanked for provision of the junglefowl. The authors thank David Gower, Kent Vliet, and David Kledzik for finding lizard and crocodile specimens for their usage and Larry Witmer for the use of his laboratory and access to CT imaging for the crocodiles. Finally, they thank Victor Ng-Thow-Hing of Honda Research Laboratory for technical assistance with the inertial properties estimation software.

LITERATURE CITED

- Alexander RMcN. 1985. Mechanics of posture and gait of some large dinosaurs. *Zool J Linn Soc* 83:1–25.
- Baca A. 1996. Precise determination of anthropometric dimensions by means of image processing methods for estimating human body segment parameter values. *J Biomech* 29:563–567.
- Bates KT, Manning PL, Hodgetts D, Sellers WI. 2009. Estimating mass properties of dinosaurs using laser scanning and 3D computer modelling. *PLoS One* 4:e4532. DOI:10.1371/journal.pone.0004532.
- Buchner HHF, Savelberg HHCM, Schamhardt HC, Barneveld A. 1997. Inertial properties of Dutch warmblood horses. *J Biomech* 30:653–658.
- Bybee PJ, Lee AH, Lamm E-T. 2006. Sizing the Jurassic theropod *Allosaurus*: assessing growth strategy and evolution of ontogenetic scaling of limbs. *J Morphol* 267:347–359.
- Carrier DR, Walter RM, Lee DV. 2001. Influence of rotational inertia on turning performance of theropod dinosaurs: clues from humans with increased rotational inertia. *J Exp Biol* 204:3717–3926.
- Cavagna GA, Heglund NC, Taylor CR. 1977. Mechanical work in terrestrial locomotion: two basic mechanisms for minimizing energy expenditure. *Am J Physiol* 233:R243–R261.
- Challis JH. 1999. Precision of the estimation of human limb inertial parameters. *J Appl Biomech* 15:418–428.
- Christiansen P, Bonde N. 2002. Limb proportions and avian terrestrial locomotion. *J Ornithol* 143:356–371.
- Clemente CJ, Withers PC, Thompson G, Lloyd D. 2008. Why go bipedal? Locomotion and morphology in Australian agamid lizards. *J Exp Biol* 211:2058–2065.
- Cott HB. 1961. Scientific results of an inquiry into the ecology and economic status of the Nile crocodile (*Crocodylus niloticus*) in Uganda and Northern Rhodesia. *Trans Zool Soc London* 29:211–358.
- Crompton RH, Li Y, Alexander RMcN, Wang W, Gunther MM. 1996. Segment inertial properties of primates: new techniques for laboratory and field studies of locomotion. *Am J Phys Anthropol* 99:547–570.
- de Leva P. 1996. Adjustments to Zatsiorsky-Seluyanov's segment inertial parameters. *J Biomech* 29:1223–1230.
- Dellanini L, Hawkins D, Martin RB, Stover S. 2003. An investigation of the interactions between lower-limb bone morphology, limb inertial properties and limb dynamics. *J Biomech* 36:913–919.
- Dempster WT, Gaughran GRL. 1967. Properties of body segments based on size and weight. *Am J Anat* 120:33–54.
- Dodson P. 1975. Functional and ecological significance of relative growth in *Alligator*. *J Zool* 175:315–355.
- Dumas R, Cheze L, Verriest J-P. 2007. Adjustments to McConville et al. and Young et al. body segment inertial parameters. *J Biomech* 40:543–553.
- Fedak MA, Heglund NC, Taylor CR. 1982. Energetics and mechanics of terrestrial locomotion. II. Kinetic energy changes of the limbs and body as a function of speed and body size in birds and mammals. *J Exp Biol* 79:23–40.
- Fumihito A, Miyake T, Sumi S-I, Takada M, Ohno S, Kondo N. 1994. One subspecies of the red junglefowl (*Gallus gallus gallus*) suffices as the matriarchic ancestor of all domestic breeds. *Proc Natl Acad Sci USA* 91:12505–12509.
- Gauthier JA, Kluge G, Rowe T. 1988. Amniote phylogeny and the importance of fossils. *Cladistics* 4:105–209.
- Goetz JE, Derrick TR, Pedersen DR, Robinson DA, Conzemius MG, Brown TD. 2008. Hip joint contact force in the emu (*Dromaius novaehollandiae*) during normal level walking. *J Biomech* 41:770–778.
- Gunga HC, Suthau T, Bellmann A, Friedrich A, Schwanebeck T, Stoinski S, Trippel T, Kirsch K, Hellwich O. 2007. Body mass estimations for *Plateosaurus engelhardti* using laser scanning and 3D reconstruction methods. *Naturwissenschaften* 94:623–630.
- Hatze H. 1980. A mathematical model for the computational determination of parameter values of anthropometric segments. *J Biomech* 13:833–843.
- Heinrich RE, Ruff CB, Weishampel DB. 1993. Femoral ontogeny and locomotor biomechanics of *Dryosaurus lettowvorbecki* (Dinosauria, Iguanodontia). *Zool J Linn Soc* 108:179–196.
- Henderson DM. 1999. Estimating the masses and centers of mass of extinct animals by 3-D mathematical slicing. *Paleobiology* 25:88–106.
- Henderson DM. 2003. Effects of stomach stones on the buoyancy and equilibrium of a floating crocodylian: a computational analysis. *Can J Zool* 81:1346–1357.
- Henderson DM. 2004. Tippy punters: sauropod dinosaur pneumaticity, buoyancy and aquatic habits. *Biol Lett* 271:180–183.
- Henderson DM. 2006. Burly gaits: centers of mass, stability, and the trackways of sauropod dinosaurs. *J Vert Paleont* 26:907–921.
- Henderson DM, Snively E. 2004. *Tyrannosaurus* en pointe: allometry minimized rotational inertia of large theropod dinosaurs. *Biol Lett* 271:S57–S60.
- Huang HK, Suarez FR. 1983. Evaluation of cross-sectional geometry and mass density distributions of humans and laboratory animals using computerized tomography. *J Biomech* 16:821–832.
- Hutchinson JR. 2004. Biomechanical modeling and sensitivity analysis of bipedal running ability. I. Extant taxa. *J Morphol* 262:421–440.
- Hutchinson JR, Ng-Thow-Hing V, Anderson FC. 2007. A 3D interactive method for estimating body segmental parameters in animals: application to the turning and running performance of *Tyrannosaurus rex*. *J Theor Biol* 246:660–680.
- Isler K, Payne RC, Gunther MM, Thorpe SKS, Li Y, Savage R, Crompton R. 2006. Inertial properties of hominoid limb segments. *J Anat* 209:201–218.
- Jensen RK. 1978. Estimation of the biomechanical properties of three body types using a photogrammetric method. *J Biomech* 11:349–358.
- Jensen RK. 1989. Changes in segment inertia proportions between 4 and 20 years. *J Biomech* 22:529–536.
- Jones TD, Farlow JO, Ruben JA, Henderson DM, Hillenius WJ. 2000. Cursoriality in bipedal archosaurs. *Nature* 406:716–718.
- Krabbe B, Farkas R, Baumann W. 1997. Influence of inertia on intersegment moments of the lower extremity joints. *J Biomech* 30:517–519.
- Lephart SA. 1984. Measuring the inertial parameters of cadaver segments. *J Biomech* 17:537–543.
- Liu Y-P, Wu G-S, Yao Y-G, Miao Y-W, Luikart G, Baig M, Beja-Pereira A, Ding Z-L, Palanichamy MG, Zhang Y-P. 2006. Multiple maternal origins of chickens: out of the Asian jungles. *Mol Phylogenet Evol* 38:12–19.
- Manion BL. 1984. The effects of size and growth on hindlimb locomotion in the chicken; Ph.D. Thesis. Chicago: University of Illinois.
- Motani R. 2001. Estimating body mass from silhouettes: testing the assumption of elliptical body cross-sections. *Paleobiology* 27:735–750.
- Mungiole M, Martin PE. 1990. Estimating segment inertial properties: comparison of magnetic resonance imaging with existing methods. *J Biomech* 23:1039–1046.
- Norton J, Donaldson N, Dekker L. 2002. 3D whole body scanning to determine mass properties of legs. *J Biomech* 35:81–86.
- Pearsall DJ, Costigan PA. 1999. The effect of body segment parameter error on gait analysis results. *Gait Posture* 9:173–183.
- Rao G, Amarantini D, Berton E, Favier D. 2006. Influence of body segments' parameters on inverse dynamics solutions during gait. *J Biomech* 39:1531–1536.

Reinbolt JA, Haftka RT, Chmielewski TL, Fregly BJ. 2007. Are patient-specific joint and inertial parameters necessary for accurate inverse dynamics analyses of gait? *IEEE Trans Biomed Eng* 54:782–793.

Reisz RR, Scott D, Sues H-D, Evans DC, Raath MA. 2005. Embryos of an early Jurassic prosauropod dinosaur and their evolutionary significance. *Science* 309:761–764.

Ren L, Hutchinson JR. 2008. The three-dimensional locomotor dynamics of African (*Loxodonta africana*) and Asian (*Elephas maximus*) elephants reveal a smooth gait transition at moderate speed. *J R Soc Interface* 5:195–211.

Sarfaty O, Ladin Z. 1993. A video-based system for the estimation of the inertial properties of body segments. *J Biomech* 26:1011–1016.

Snively E, Russell AP. 2007. Craniocervical feeding dynamics of *Tyrannosaurus rex*. *Paleobiology* 33:610–638.

Srygley RB, Dudley R. 1993. Correlation of the position of body center of mass with butterfly escape tactics. *J Exp Biol* 174:155–166.

van den Bogert AJ, Schamhardt HC, Crowe A. 1989. Simulation of quadrupedal locomotion using a dynamic rigid body model. *J Biomech* 22:33–41.

Walter RM, Carrier DR. 2002. Scaling of rotational inertia in murine rodents and two species of lizard. *J Exp Biol* 205:2135–2141.

Webb GJW, Messel H. 1978. Morphometric analysis of *Crocodylus porosus* from the north coast of Arnhem land, northern Australia. *Aust J Zool* 26:1–27.

Wei C, Jensen RK. 1995. The application of segment axial density profiles to a human body inertia model. *J Biomech* 28:103–108.

Wicke J, Dumas GA, Costigan PA. 2008. Trunk density profile estimates from dual x-ray absorptiometry. *J Biomech* 41:861–867.

Yeadon MR. 1990. The simulation of aerial movement—II. A mathematical inertia model of the human body. *J Biomech* 23:67–74.

Zatsiorsky V, Seluyanov V. 1983. The mass and inertia characteristics of the main segment of the human body. In: Matsui K, Kobayashi K, editors. *Biomechanics VIII-B*. Campaign, IL: Human Kinetics Publishers. p 1152–1159.

Zug G. 1974. Crocodilian galloping: an unique gait for reptiles? *Copeia* 2:550–552.

APPENDIX

TABLE A1. Chicken inertial properties

Subject	Body mass (kg)	Body mass estimate (kg)	Body mass estimate with legs removed (kg)	Femur length (m)	Limb length (m)	Body length (m)	Body COM			Inertial tensor (kg m ⁻²)—body		
							COM coordinates			x	y	z
Low resolution												
Juvenile broiler 1	1.789	1.898	1.330	0.074	0.247	0.365	0.050	0.032	-0.018	0.004	0.013	0.012
Juvenile broiler 2	2.031	2.117	1.535	0.066	0.242	0.382	0.046	0.025	-0.030	0.004	0.018	0.015
Juvenile broiler 3	1.831	1.925	1.374	0.071	0.244	0.356	0.043	0.027	-0.030	0.004	0.013	0.011
Juvenile broiler 4	2.119	2.205	1.624	0.076	0.254	0.373	0.044	0.025	-0.033	0.005	0.017	0.014
Juvenile broiler 5	1.972	2.140	1.565	0.071	0.241	0.371	0.040	0.031	-0.025	0.004	0.015	0.013
Juvenile broiler 6	1.853	1.881	1.300	0.075	0.247	0.338	0.045	0.027	-0.013	0.004	0.012	0.010
Juvenile broiler 7	2.043	2.063	1.511	0.075	0.259	0.361	0.043	0.031	-0.020	0.004	0.015	0.013
Juvenile broiler 8	2.086	2.192	1.532	0.073	0.259	0.359	0.045	0.030	-0.026	0.004	0.016	0.014
Juvenile broiler 9	1.869	1.853	1.341	0.068	0.238	0.344	0.040	0.027	-0.027	0.004	0.013	0.011
Juvenile broiler 10	2.308	2.290	1.615	0.071	0.249	0.375	0.043	0.034	-0.026	0.005	0.019	0.016
Mature broiler 1	3.106	3.354	2.430	0.080	0.270	0.39334	0.039	0.042	-0.033	0.009	0.032	0.027
Mature broiler 2	2.896	3.107	2.265	0.077	0.268	0.38295	0.032	0.050	-0.025	0.003	0.027	0.023
Mature broiler 3	2.578	2.687	1.834	0.081	0.271	0.38474	0.035	0.037	-0.035	0.006	0.019	0.017
Mature broiler 4	2.763	2.844	2.003	0.075	0.253	0.41191	0.047	0.037	-0.025	0.007	0.026	0.022
Mature broiler 5	2.587	2.626	1.923	0.077	0.260	0.39292	0.042	0.041	-0.019	0.006	0.020	0.023
Juvenile junglefowl 1	0.698	0.737	0.531	0.066	0.226	0.305	0.032	0.027	-0.005	0.001	0.004	0.003
Juvenile junglefowl 2	0.629	0.748	0.583	0.064	0.219	0.305	0.021	0.036	-0.018	0.001	0.004	0.004
Juvenile junglefowl 3	0.523	0.548	0.423	0.061	0.203	0.257	0.015	0.034	-0.002	0.000	0.003	0.003
Juvenile junglefowl 4	0.531	0.578	0.448	0.061	0.207	0.274	0.031	0.026	-0.016	0.001	0.002	0.002
Juvenile junglefowl 5	0.632	0.703	0.488	0.064	0.215	0.293	0.020	0.035	-0.020	0.001	0.003	0.003
Junglefowl 1	1.972	2.145	1.645	0.092	0.318	0.426	0.040	0.044	-0.030	0.004	0.020	0.018
Junglefowl 2	2.073	2.550	1.610	0.093	0.328	0.444	0.050	0.046	-0.026	0.004	0.019	0.018
Junglefowl 3	2.069	2.283	1.656	0.094	0.330	0.442	0.051	0.034	-0.045	0.004	0.021	0.019
Junglefowl 4	1.708	1.851	1.417	0.088	0.321	0.428	0.054	0.044	-0.019	0.003	0.017	0.016
Junglefowl 5	1.872	2.019	1.470	0.093	0.331	0.422	0.050	0.046	-0.015	0.004	0.018	0.016
High resolution												
Mature broiler 4	2.763	2.853	Not calculated	0.075	0.253	0.41191	0.039	0.039	-0.027	0.007	0.027	0.023
Junglefowl 5	1.872	2.005		0.093	0.331	0.422	0.050	0.043	-0.014	0.004	0.018	0.016
Repeated measures												
Mature broiler 1	3.106	3.088	Not calculated	0.080	0.270	0.39334	0.039	0.041	-0.031			
Mature broiler 2	2.896	2.975		0.077	0.268	0.38295	0.026	0.037	-0.035			
Mature broiler 3	2.578	2.682		0.081	0.271	0.38474	0.037	0.038	-0.028	Not calculated		
Mature broiler 4	2.763	2.785		0.075	0.253	0.41191	0.038	0.044	-0.035			
Mature broiler 5	2.587	2.594		0.077	0.260	0.39292	0.039	0.045	-0.027			

x, cranial; y, ventral; z, medial.

TABLE A2. Chicken inertial properties (trunk)

Subject	Trunk COM			Inertial tensor (kg m ⁻²)—trunk		
	COM coordinates			x	y	z
	x	y	z			
Low resolution						
Juvenile broiler 1	0.073	0.032	-0.019	0.002	0.008	0.007
Juvenile broiler 2	0.071	0.023	-0.028	0.002	0.010	0.009
Juvenile broiler 3	0.065	0.027	-0.032	0.002	0.007	0.007
Juvenile broiler 4	0.067	0.024	-0.032	0.002	0.010	0.009
Juvenile broiler 5	0.063	0.029	-0.026	0.002	0.009	0.008
Juvenile broiler 6	0.067	0.024	-0.013	0.002	0.007	0.006
Juvenile broiler 7	0.064	0.030	-0.020	0.002	0.009	0.008
Juvenile broiler 8	0.069	0.029	-0.026	0.002	0.010	0.009
Juvenile broiler 9	0.059	0.025	-0.027	0.002	0.007	0.007
Juvenile broiler 10	0.068	0.029	-0.030	0.002	0.011	0.010
Mature broiler 1	0.067	0.041	-0.033	0.005	0.018	0.016
Mature broiler 2	0.055	0.049	-0.025	0.004	0.015	0.014
Mature broiler 3	0.058	0.037	-0.034	0.003	0.012	0.011
Mature broiler 4	0.073	0.038	-0.023	0.004	0.016	0.014
Mature broiler 5	0.068	0.039	-0.022	0.003	0.013	0.012
Juvenile junglefowl 1	0.050	0.027	-0.005	0.002	0.002	0.000
Juvenile junglefowl 2	0.043	0.034	-0.019	0.002	0.002	0.000
Juvenile junglefowl 3	0.037	0.032	-0.002	0.001	0.001	0.000
Juvenile junglefowl 4	0.047	0.025	-0.014	0.001	0.001	0.000
Juvenile junglefowl 5	0.044	0.034	-0.019	0.002	0.002	0.000
Junglefowl 1	0.064	0.042	-0.030	0.003	0.012	0.012
Junglefowl 2	0.073	0.046	-0.026	0.003	0.012	0.012
Junglefowl 3	0.076	0.031	-0.043	0.003	0.013	0.012
Junglefowl 4	0.078	0.042	-0.021	0.002	0.011	0.010
Junglefowl 5	0.071	0.044	-0.018	0.002	0.011	0.010
High Resolution						
Mature broiler 4	Not calculated			Not calculated		
Junglefowl 5						
Repeated measures						
Mature broiler 1						
Mature broiler 2						
Mature broiler 3	Not calculated			Not calculated		
Mature broiler 4						
Mature broiler 5						

x, cranial; y, ventral; z, medial.

TABLE A3. Complex, standard, and informed models of Juvenile *Crocodylus johnstoni*

Model iteration	Body mass (kg)	Body mass estimate (kg)	Femur length (m)	Gleno-Acetabular length (m)	COM coordinates (m)		
					x	y	z
Complex model, original pose, with cavities	1.540	1.722	0.054	0.177	0.025	-0.014	-0.018
Complex model, original pose, without cavities	1.540	1.791	0.054	0.177	0.030	-0.013	-0.018
Complex model, original pose, raw scan without cavities	1.540	1.790	0.054	0.177	0.027	-0.011	-0.020
Complex model, straightened pose, with cavities	1.540	1.817	0.054	0.177	0.047	-0.013	-0.021
Complex model, straightened pose, without cavities	1.540	1.858	0.054	0.177	0.050	-0.013	-0.022
Complex model, straightened torso only with cavities	0.789	0.789	0.054	0.177	0.089	-0.012	-0.021
Complex model, straightened torso only without cavities	0.789	0.824	0.054	0.177	0.089	-0.012	-0.022
Simple model, standard tail, maximum total body mass	1.540	1.726	0.054	0.177	0.083	-0.014	-0.022
Simple model, standard tail, minimum total body mass	1.540	0.952	0.054	0.177	0.099	-0.014	-0.023
Simple model, standard tail, maximum cranial distribution of mass	1.540	1.560	0.054	0.177	0.100	-0.014	-0.022
Simple model, standard tail, maximum caudal distribution of mass	1.540	1.132	0.054	0.177	0.073	-0.015	-0.022
Simple model, standard tail, maximum dorsal distribution of mass	1.540	1.668	0.054	0.177	0.086	-0.013	-0.022
Simple model, standard tail, maximum ventral distribution of mass	1.540	1.024	0.054	0.177	0.092	-0.016	-0.022
Mean of standard tail models	1.540	1.346	0.054	0.177	0.087	-0.015	-0.022
Simple model, informed tail, maximum total body mass	1.540	1.983	0.054	0.177	0.055	-0.014	-0.022
Simple model, informed tail, minimum total body mass	1.540	1.067	0.054	0.177	0.075	-0.014	-0.023
Simple model, informed tail, maximum cranial distribution of mass	1.540	1.675	0.054	0.177	0.084	-0.013	-0.022
Simple model, informed tail, maximum caudal distribution of mass	1.540	1.389	0.054	0.177	0.034	-0.015	-0.022
Simple model, informed tail, maximum dorsal distribution of mass	1.540	1.926	0.054	0.177	0.056	-0.013	-0.022
Simple model, informed tail, maximum ventral distribution of mass	1.540	1.139	0.054	0.177	0.070	-0.016	-0.022
Mean of informed tail models	1.540	1.532	0.054	0.177	0.059	-0.015	-0.022

x, cranial; y, ventral; z, medial.

TABLE A4. Complex, standard, and informed models of adult *Crocodylus johnstoni*

Model iteration	Body mass (kg)	Body mass estimate (kg)	Femur length (m)	Gleno-Acetabular length (m)	COM coordinates (m)		
					x	y	z
Complex model, original pose, with cavities	20.190	20.935	0.105	0.421	0.155	0.009	-0.102
Complex model, original pose, without cavities	20.190	21.767	0.105	0.421	0.164	0.010	-0.101
Complex model, original pose, raw scan without cavities	20.190	21.258	0.105	0.421	0.160	0.009	-0.101
Complex model, straightened pose, with cavities	20.190	21.090	0.105	0.421	0.119	-0.012	-0.053
Complex model, straightened pose, without cavities	20.190	21.888	0.105	0.421	0.129	-0.011	-0.053
Complex model, straightened torso only with cavities	11.058	11.058	0.105	0.421	0.200	0.000	-0.053
Complex model, straightened torso only without cavities	11.058	11.684	0.105	0.421	0.204	0.001	-0.053
Simple model, standard tail, maximum total body mass	20.190	22.718	0.105	0.421	0.178	-0.013	-0.056
Simple model, standard tail, minimum total body mass	20.190	11.992	0.105	0.421	0.198	-0.015	-0.058
Simple model, standard tail, maximum cranial distribution of mass	20.190	20.476	0.105	0.421	0.213	-0.010	-0.056
Simple model, standard tail, maximum caudal distribution of mass	20.190	14.375	0.105	0.421	0.142	-0.021	-0.056
Simple model, standard tail, maximum dorsal distribution of mass	20.190	21.863	0.105	0.421	0.185	-0.010	-0.055
Simple model, standard tail, maximum ventral distribution of mass	20.190	13.030	0.105	0.421	0.181	-0.021	-0.058
Mean of standard tail models	20.190	17.436	0.105	0.421	0.178	-0.016	-0.056
Simple model, informed tail, maximum total body mass	20.190	26.000	0.105	0.421	0.122	-0.017	-0.053
Simple model, informed tail, minimum total body mass	20.190	13.458	0.105	0.421	0.149	-0.016	-0.056
Simple model, informed tail, maximum cranial distribution of mass	20.190	21.942	0.105	0.421	0.182	-0.011	-0.055
Simple model, informed tail, maximum caudal distribution of mass	20.190	17.657	0.105	0.421	0.066	-0.025	-0.053
Simple model, informed tail, maximum dorsal distribution of mass	20.190	25.145	0.105	0.421	0.126	-0.014	-0.053
Simple model, informed tail, maximum ventral distribution of mass	20.190	14.496	0.105	0.421	0.137	-0.022	-0.056
Mean of informed tail models	20.190	19.810	0.105	0.421	0.124	-0.018	-0.054

x, cranial; y, ventral; z, medial.

TABLE A5. Complex, standard, and informed models of adult Junglefowl (*Gallus gallus*)

Model iteration	Body mass (kg)	Body mass estimate (kg)	Femur length (m)	Gleno-Acetabular length (m)	COM coordinates (m)		
					x	y	z
Complex model, original pose, with maximally inflated cavities	2.069	2.141	0.087	0.136	0.092	-0.026	-0.012
Complex model, original pose, with minimally inflated cavities	2.069	2.435	0.087	0.136	0.087	-0.023	-0.012
Mean of complex models, original poses with varying inflation	2.069	2.288	0.087	0.136	0.090	-0.025	-0.012
Complex model, original pose, without cavities	2.069	2.717	0.087	0.136	0.086	-0.019	-0.013
Complex model, original pose, raw scan without cavities	2.069	2.710	0.087	0.136	0.097	-0.030	-0.013
Complex model, straightened pose, with maximally inflated cavities	2.069	2.537	0.087	0.136	0.065	-0.048	-0.025
Complex model, straightened pose, with minimally inflated cavities	2.069	2.815	0.087	0.136	0.063	-0.045	-0.024
Mean of complex models, straightened poses with varying inflation	2.069	2.676	0.087	0.136	0.064	-0.047	-0.025
Complex model, straightened pose without cavities	2.069	3.065	0.087	0.136	0.062	-0.042	-0.025
Complex model, straightened torso only, with maximally inflated cavities	1.544	1.025	0.087	0.136	0.047	-0.033	-0.027
Complex model, straightened torso only, with minimally inflated cavities	1.544	1.303	0.087	0.136	0.046	-0.030	-0.026
Complex model, straightened torso only, without cavities	1.544	1.544	0.087	0.136	0.047	-0.027	-0.026
Simple model, standard tail, maximum total body mass	2.069	3.659	0.087	0.136	0.053	-0.053	-0.021
Simple model, standard tail, minimum total body mass	2.069	1.943	0.087	0.136	0.059	-0.052	-0.025
Simple model, standard tail, maximum cranial distribution of mass	2.069	3.104	0.087	0.136	0.065	-0.041	-0.022
Simple model, standard tail, maximum caudal distribution of mass	2.069	2.594	0.087	0.136	0.044	-0.066	-0.025
Simple model, standard tail, maximum dorsal distribution of mass	2.069	3.119	0.087	0.136	0.064	-0.041	-0.022
Simple model, standard tail, maximum ventral distribution of mass	2.069	2.588	0.087	0.136	0.043	-0.065	-0.023
Mean of standard tail models	2.069	2.851	0.087	0.136	0.054	-0.053	-0.023

x, cranial; y, ventral; z, medial.